
Article:
Pitruzzello, Giampaolo, Conteduca, Donato and Krauss, Thomas F. orcid.org/0000-0003-4367-6601 (2020) Nanophotonics for bacterial detection and antimicrobial susceptibility testing. Nanophotonics. ISSN 2192-8614

https://doi.org/10.1515/nanoph-2020-0388

Review

Giampaolo Pitruzzello*, Donato Conteduca and Thomas F. Krauss

Nanophotonics for bacterial detection and antimicrobial susceptibility testing

https://doi.org/10.1515/nanoph-2020-0388
Received July 21, 2020; accepted August 27, 2020; published online September 17, 2020

Abstract: Photonic biosensors are a major topic of research that continues to make exciting advances. Technology has now improved sufficiently for photonics to enter the realm of microbiology and to allow for the detection of individual bacteria. Here, we discuss the different nanophotonic modalities used in this context and highlight the opportunities they offer for studying bacteria. We critically review examples from the recent literature, starting with an overview of photonic devices for the detection of bacteria, followed by a specific analysis of photonic antimicrobial susceptibility tests. We show that the intrinsic advantage of matching the optical probed volume to that of a single, or a few, bacterial cell, affords improved sensitivity while providing additional insight into single-cell properties. We illustrate our argument by comparing traditional culture-based methods, which we term macroscopic, to microscopic free-space optics and nanoscopic guided-wave optics techniques. Particular attention is devoted to this last class by discussing structures such as photonic crystal cavities, plasmonic nanostructures and interferometric configurations. These structures and associated measurement modalities are assessed in terms of limit of detection, response time and ease of implementation. Existing challenges and issues yet to be addressed will be examined and critically discussed.

Keywords: antimicrobial resistance; bacteria; evanescent-wave sensing; photonic biosensors.

***Corresponding author: Giampaolo Pitruzzello**, Department of Physics, University of York, Heslington, YO10 5DD, York, UK, E-mail: giampaolo.pitruzzello@york.ac.uk. https://orcid.org/0000-0002-8030-7699
Donato Conteduca and Thomas F. Krauss, Department of Physics, University of York, Heslington, YO10 5DD, York, UK, E-mail: donato.conteduca@york.ac.uk (D. Conteduca), thomas.krauss@york.ac.uk (T.F. Krauss)

1 Introduction

Bacteria are ubiquitous in nature. As much as they are vital for our survival and the balance of any ecosystem, they can also be harmful and pose serious risks in areas such as health care, food, or environmental security [1–4]. Therefore, the detection and monitoring of bacteria are key challenges, with time to result and sensitivity being major drivers. This is especially true in health care applications, where antimicrobial resistance (AMR) is a key issue and where the slowness of current antimicrobial susceptibility tests (ASTs) prevents timely and specific drug prescription [4–6].

Traditional microbiological techniques for detecting and studying bacteria are culture-based, whereby bacteria are grown on a substrate, such as an agar plate, for visual inspection. These techniques are labour-intensive, time-consuming, and difficult to conduct outside a specialized microbiology laboratory. Another crucial limitation of traditional tests is that they examine billions of microorganisms at once, thereby washing out cellular individuality and heterogeneity; the outcome is a single value within a confidence interval, which then disregards any underlying distribution of quantities of interest. Bacterial populations, however, are strongly heterogeneous and cell-to-cell differences are crucial in a variety of phenomena, such as the development of antibiotic heteroresistance [7–9] or persistence [7, 10]. In addition, there is growing evidence that the heterogeneity of bacterial colonies is a key factor in determining the failure of an antibiotic therapy [11, 12]. Consequently, an ideal AST must be able to discern the signature(s) of susceptibility to the antibiotic at low concentrations of bacteria by characterizing their response at the single bacteria level, with the twofold aim of speeding up detection and probing the heterogeneity of the bacterial population [13–15]. Novel optical and photonic detection modalities have recently emerged to address this challenge. Photonic sensors exploit the interaction of guided light with bacteria to detect their presence and probe their response, whereby the use of light offers key advantages, such as immunity to external electromagnetic interferences that may disturb sensors operating in other regions of the electromagnetic

spectrum [16], and ease of parallel, high-sensitivity and noncontact detection.

Optical sensors can be divided into fluorescence-based and label-free devices. To date, most light-based sensors use fluorescence, whereby target molecules, such as those on the bacterial cell wall, are labelled with fluorophores to indicate the presence, concentration and activity of bacteria [17]. While a comprehensive comparison between fluorescence-based and label-free sensors is beyond the scope of this article, we note that the former is extremely sensitive, selective and easily able to reach singe-cell resolution. On the other hand, fluorescent labelling complicates procedures, can interfere with bacterial viability and requires prior knowledge of the bacteria to be labelled [18, 19]. We therefore focus on label-free techniques. In addition, biosensors can be divided into two further groups: those detecting target bacterial components, such as genetic material or specific enzymes and those based on whole cell detection [2]. The former class requires further sample processing to extract and purify the target material, such as cell lysis, which inevitably increases process time and complexity. Hence here, in the interest of simplicity, we focus on label-free whole-bacteria detection techniques that guide, confine or mould light with nanostructures.

1.1 The role and advantages of photonic in bacterial detection and ASTs

Photonic sensors achieve their functionality by exploiting enhanced light-matter interaction, tight mode confinement and extreme phase sensitivity. Photonic sensors are typically based on guided modes and interact with the analyte via their evanescent tail. The overlap integral (OI) quantifies the fraction of the mode's electric field intensity $|\boldsymbol{E}(\boldsymbol{r})|^2$ overlapping with the cladding material to be sensed and can be expressed as

$$\mathrm{OI} = \frac{\int_{V_{\mathrm{clad}}} \varepsilon(\boldsymbol{r})|\boldsymbol{E}(\boldsymbol{r})|^2 d^3\boldsymbol{r}}{\int_{V_{\mathrm{tot}}} \varepsilon(\boldsymbol{r})|\boldsymbol{E}(\boldsymbol{r})|^2 d^3\boldsymbol{r}}$$

The integration is carried out over the cladding volume above the sensor surface (V_{clad}) and the total volume of the mode (V_{tot}), while $\varepsilon(\boldsymbol{r})$ represents the spatial dependency of the dielectric constant. This integral is therefore a key determinant of the bulk sensitivity of the method. Larger values of the OI correspond to a larger overlap of the field with the sensing medium leading, in turn, to a bigger change of the effective index of the mode for a given change of the refractive index of the cladding. All sensors based on surface plasmons and those based on dielectric waveguides are based on this principle.

The extent of the evanescent tail determines the interaction volume, and is easily obtained from guided-mode theory via the decay constant γ:

$$\gamma = \frac{2\pi}{\lambda}\sqrt{n_{\mathrm{eff}}^2 - n_c^2}$$

where n_{eff} is the effective index of the optical mode, n_c is the refractive index of the cladding (typically water, i.e. $n_c \sim 1.33$) and λ the wavelength. Considering that the effective index is 1.5–1.7 for a plasmonic mode and 1.5–2.5 for a dielectric mode, the typical decay length $1/\gamma$ in water-based claddings is in the range of 100–200 nm [20].

These values of γ imply that because the interaction with surface-attached bacteria only occurs via the evanescent tail of the mode, the probed volume is limited to the bacterial membrane and its immediate vicinity inside the cell. The limited penetration of the optical mode also means that background interference, for example, from bacteria and media further away from the surface, is minimized, making for good signal to noise ratios. Therefore, photonic structures naturally offer themselves as good candidates for the sensing of single or small numbers of bacteria.

In addition, such a localized interaction makes nanophotonic structures able to probe different bacterial properties. For example, different bacterial strains have different optical density (OD) of the cell wall, therefore enabling identification [21, 22]; the OD of the membrane may change as a result of an antibiotic challenge which manifests itself as a change in refractive index [23]; the motion of bacteria is an indicator for their metabolic activity and is manifested as readout noise [24, 25]; the morphology of the cell may be affected by antibiotics and will impact on its light scattering properties [26]. In any of these cases, the increased sensitivity offered by nanophotonic structures can allow for individual bacteria to be detected and analysed.

It is important to note that because bacteria need to be exposed to the evanescent tail of the confined mode to be detected and analysed, the sensor surface is often coated with biorecognition elements, such as antibodies, aptamers or bacteriophages that selectively bind to proteins in the bacterial membrane [27]. In addition, optical biosensors often rely on microfluidic methods to deliver the analyte to the sensing area [28]. The use of microfluidics comes with the attractive advantage of reducing the required volume of solution while decreasing the characteristic length and diffusion time needed for bacteria to reach and attach to the sensor's surface [29, 30]. While a thorough description of these aspects is outside the scope of this review, we note that both the surface chemistry and the microfluidics are key

factors in determining the overall performance of a sensor. This is especially true for the detection time, which depends on the dimension of the respective fluidic cell, as surface affinity binding is fundamentally driven by diffusion, but also the quality of the surface receptor layers and the binding affinity to the bacteria of interest.

Even though the recent literature is rich with examples of photonic biosensing platforms, we believe that the potential of photonics in this space has not yet been fully exploited. To this end, we wish to present some of the most relevant recent work to provide a critical assessment of the state of the art and to highlight the key advantages of photonic techniques for the detection and study of single bacteria, especially in the context of AMR.

The review is divided into two major sections. In Section 2, we discuss different methods for detecting and imaging bacteria, mainly focussing on evanescent wave nanophotonic sensors. Section 3 describes the different photonic methods used for studying the susceptibility of bacteria to antibiotics. To highlight the benefits of light confinement, we discuss techniques in order of progressive reduction of the optically probed volume. We start with traditional culture-based methods, such as the disk diffusion test, which we term macroscopic, then move on to microscopic free-space optical and nanoscopic guided-wave optical methods. While macroscopic techniques are based on averaging cellular growth over the entire bacterial population, microscopic free-space optics methods such as bulk optical tweezers, elastic light scattering, flow cytometry and some nanostructure-based techniques afford probing fewer bacteria, even down to single cells, but still retrieve information from the entire cell. Conversely, nanoscopic techniques such as surface plasmon resonances (SPRs), guided mode resonances (GMRs) or metasurfaces-based configurations rely on guided-wave optics and exploit the evanescent wave at interfaces, as described previously. The optical field is now confined to the surface of the sensor so that only the bacterial membrane is probed. Some of the nanoscopic techniques also exploit resonant enhancement which further increases sensitivity [21, 23, 31, 32]. Overall, we show that this reduction in volume enables gaining further insight into bacterial behaviour, as well as increasing sensitivity and reducing the time needed to assess antibiotic action.

2 Photonics for bacterial detection

In terms of detection and observation, macroscopic and microscopic techniques require little introduction; the first bacteria were observed with a microscope by van Leeuwenhoek in 1677 [33]. We therefore move straight to nanophotonic techniques used to detect and image bacteria at very low concentrations, down to the single cell level. We classify the structures into two main categories: plasmonic and dielectric (See Tables 1 and 2), and we discuss them with particular attention to the optically probed volume relative to the volume of a single bacterial cell. We also discuss the current limitations of nanophotonics for bacterial studies to highlight potential future research directions.

2.1 Plasmonic configurations

2.1.1 SPR devices

Plasmonic biosensors typically consist of metallic thin films which support SPRs and which strongly confine light at the interface between the thin metal film and the analyte. Using surface functionalization techniques, the metal layer then allows to selectively bind biomarkers or cells of interest. SPRs are typically excited using the Kretschmann configuration, whereby light is injected through a prism and any changes in refractive index result in a change of resonance angle, wavelength, or intensity. SPR was the first label-free photonic detection technique to be commercialized (by Biacore, now GE Healthcare).

More recently, SPR sensors have also been used for the detection and imaging of bacteria. SPR offers a particularly high surface sensitivity, both because of the strong overlap of the evanescent field with the analyte and because of its peculiar mode coupling properties [34, 35], which allows for the detection of very low concentrations of bacteria, that is, down to 10^2–10^3 CFU/mL (colony-forming units) in $t \sim 20$ min [36]. It is important to note that the detection time is not limited by the detection principle, but it depends on other factors such as the surface functionalization protocol and is influenced by the quality of the bioreceptor layer and its binding affinity to the target bacterium.

Several sensing techniques have been used to further improve the sensitivity of plasmonic configurations, for example, by imprinting bacteria in soft polymers on metal slabs or by using metal nanoparticles to enhance the changes of reflectivity on bacterial binding [37]. However, even if these sensing schemes provide an Limit Of Detection (LOD) < 1 CFU/mL, their main issue is the need for a rather complex and slow preparation process (>24 h), which makes them less ideal for rapid diagnosis and commercialization, therefore impacting on the attractiveness of the approach.

A simpler SPR measurement scheme is offered by crossed surface relief gratings (CSRGs), which consist of

two orthogonally superimposed dielectric gratings covered by a thin metal layer. One of the gratings provides the necessary wavevector to excite the plasmon wave if the incident field is polarized along the grating vector. Energy is then exchanged between the two gratings, such that light is radiated by the second grating with a polarization orthogonal to the incident one. Therefore, if the CSRG is placed between two cross polarizers and illuminated by broadband light, a peak in the transmission spectrum is observed and used for biosensing. This principle enabled to simplify the optical setup compared to traditional SPR, even though more modest LODs were achieved ($<10^5$ CFU/mL for *Escherichia coli*) [38].

2.1.2 Plasmonic nanohole arrays

An alternative way of exciting surface plasmons is to use grating-coupling instead of the prism-coupling method used in the Kretschmann configuration. The grating-coupling method is best embodied by the nanohole array (NHA) geometry, that is, a periodic distribution of subwavelength apertures [39]. These subwavelength apertures both enable easy out-of-plane coupling and they support the phenomenon of enhanced optical transmission at resonance which leads to a significant energy enhancement in the nanoapertures [40]. The ease of light-coupling and the compatibility with cost-effective optical components (e.g. LED sources) also makes for an easy implementation. Although the bulk sensitivity of plasmonic nanostructures is typically lower than that of prism-coupled SPR sensors [34, 35], the strong light confinement in the nanoapertures improves surface sensitivity and spatial resolution. These features have been shown to be beneficial to biochemical sensing, whereby plasmonic nanoholes have achieved low limits of detection for proteins. More recently, applications in bacterial detection have also emerged [31, 41, 42].

For example, Gomez-Cruz et al. [42] demonstrated the detection of low concentrations of uropathogenic *E. coli* in urine by using a plasmonic nanohole array with intensity-based measurements in only 15 min. The sensor exhibits an LOD of 100 CFU/mL, which is comparable with other plasmonic techniques [36]. Notably, the authors achieved detection with an analyte volume as small as 10 µL, which means that, on average, only a single bacterium was present and detected. A similar performance was achieved by Dey et al. with an NHA configuration combined with an interferometric approach [31] where the interference between two spatially separated, orthogonally polarized beams was measured. Measuring the relative difference between two collinear beams, rather than the absolute change of an individual one, minimizes the impact of mechanical, thermal, and optical source noise, which we have recently shown to be advantageous also for protein measurements [43].

In the context of this review, we note that the aforementioned interferometric approach enabled the detection of a single *E. coli* bacterium in a volume of 10 µL of diluted blood plasma [31]. This corresponds to an LOD = 100 CFU/mL, which is the same as that achieved with the intensity-based sensor by Gomez-Cruz et al. mentioned previously [42]. Nevertheless, it is important to note that the interferometric device was realized in a handheld format, where the noise level is typically higher than in an optical benchtop experiment. The higher sensitivity of interferometry therefore compensates for the higher noise, which has led to the detection of a single bacterium with a portable instrument and represents a notable proof of concept for the translation of a nanoplasmonic device into the medical environment.

2.1.3 Plasmonic imaging

SPR sensors have been also used for the imaging of biological samples, such as cells and bacteria. This prism-based SPR imaging (SPRi) method exploits both the angular and the wavelength response of a fixed input beam to generate the image and the sensing information [44]. Using this method, Bouguelia et al. [45] have demonstrated the detection of less than 20 CFU/mL of *E. coli* with a prism-based SPRi system. However, a limitation of prism-based SPRi is that the image plane is not perpendicular to the optical axis of the system, which creates a skew between the camera and the sensor surface. Only a narrow band is in focus in the image with a consequent worsening of resolution [46, 47], which severely limits the field of view.

A solution to the skew issue was introduced by Boulade et al. [46], who developed a resolution-optimized surface plasmon resonance imaging (RO-SPRi). The method consists of capturing multiple images in different focal planes to overcome the skew between the camera image plane and the sensor surface. The RO-SPRi system enabled imaging of individual *Listeria monocytogenes* and *Listeria innocua* bacteria and made them clearly visible with a field of view of 1.5 mm^2. In a direct comparison with differential interference contrast microscopy, they also showed that, not only SPRi managed to achieve a comparable field of view, but it also provided a higher accuracy in picking out bacteria on the sensor surface because it is based on evanescent fields rather than on Gaussian beams.

This higher accuracy only refers to the vertical axis, however. In the lateral dimension, the resolution is limited by the propagation length of the plasmon wave, which is typically of order 5–10 µm, so larger than the dimension of

a typical bacterium. Nevertheless, by using relatively short wavelengths (e.g. 530 nm) or lossy substrates (e.g. aluminium) [48, 49], the propagation length can be reduced significantly. A different strategy for improving the lateral resolution consists of using an objective-based SPRi [50], whereby the need for the prism typical of the traditional Kretschmann configuration is eliminated by launching the SPR through a high numerical aperture (NA) immersion objective. Eliminating the physical constraints of the prism allows for higher NA and magnification to be achieved and, therefore, for spatial resolution to be increased. Indeed, this technique enabled the imaging of individual *E. coli* [51], of single influenza viruses [52], the mapping of proteins within mammalian cell membranes [53] and the tracking of organelles within a cell body [54]. These results confirm the suitability of SPRi for the nanoscopic analysis of bacteria and viruses as long as the limitations of the technique are understood and suitably addressed.

As an alternative, CSRGs have also been used for the SPRi of bacteria. Even though the resonant information was not in resolved spatially, Nair et al. obtained an LOD of 100 CFU/mL for *E. coli* by measuring the intensity changes induced by bacterial binding onto CSRGs [55].

2.1.4 Plasmonic nanotweezers

Plasmonic nanostructures have also been used to trap bacteria using optical forces. The pioneering studies of Ashkin et al. [56, 57] already demonstrated the contact-free trapping of single *E. coli* bacteria with a laser beam. Nevertheless, trapping required optical powers of tens of milliwatts, which rendered the bacteria inviable after only a few minutes because of photodamage [56]. The issue of photodamage can be overcome by resorting to near-field techniques that offer a stronger field gradient, which leads to stronger trapping forces even at low power. In fact, the trapping action is directly proportional to the gradient force, and therefore proportional to the gradient of the electric field, while the scattering and the absorption forces are proportional to the light intensity. As a result, nanoscale confinement affords strong trapping forces because of the strong gradient field generated in the near-field even with limited input power while limiting the contributions of scattering and absorption [58].

The trapping of bacteria in the near-field was then demonstrated by Lotan et al. [59] who fabricated nanoscale plasmonic V-groove waveguides as shown in Figure 1(a). The modes of these waveguides exert strong optical forces on objects in their proximity, which was verified by collecting the fluorescence signal from labelled bacteria (see Figure 1(b) and (c)). Even more impressively, trapping of single proteins was demonstrated with a gold double-nanohole structure [60], which confirms the suitability of near-field techniques for the trapping of nanoscale objects, given that optical forces scale with the volume of the object [58].

Exploiting resonant enhancement, plasmonic nanostructures have been used by Righini et al. [61], who achieved the trapping of several individual bacteria simultaneously in an array of dipole nanoantennas (see schematic in Figure 1(d)). Stable confinement with a trapping time of several hours was observed with a power density of about 10^8 W/m^2, or 0.1 mW/μm^2. This value is almost two orders of magnitude lower than SPR-based plasmonic tweezers and much lower than the damage threshold values for bacteria, which is typically quoted as 10^{10} W/m^2, or 10 mW/μm^2 [62, 63]. Examples of trapped bacteria are shown in Figure 1(f). This achievement clearly highlights the benefits of resonant enhancement and near-field trapping and confirm the advantages offered by nanostructured tweezers for the detection and manipulation of individual bacteria. In addition, thanks to the arraying capability of several individual cells over time, these nanotweezers may enable further studies of the time-dependence of the bacterial response to drugs, which will be further discussed in Section 3.

2.2 Dielectric configurations

Dielectric configurations have been investigated more recently with a view to overcoming the limitations arising from the intrinsic optical losses of plasmonic systems [20, 64, 65]. Dielectric materials are typically transparent in the visible and near-IR range, thereby minimizing absorption and reducing thermal effects due to Joule heating. Similar to their plasmonic counterpart, dielectric structures are refractive index sensors that interact with the analyte via the evanescent tail of the mode they support, meaning that they may also enable probing the bacteria nanoscopically. However, unlike plasmonic devices, dielectric structures can support resonances with higher dynamic range, because of the lower loss, which improves the signal-to-noise ratio and, in principle, makes it easier to detect small objects such as bacteria.

2.2.1 Optical waveguides and interferometric approaches

Sensors based on optical waveguides were the first dielectric configurations to be used for bacterial detection [66]. These waveguides detect the phase change incurred

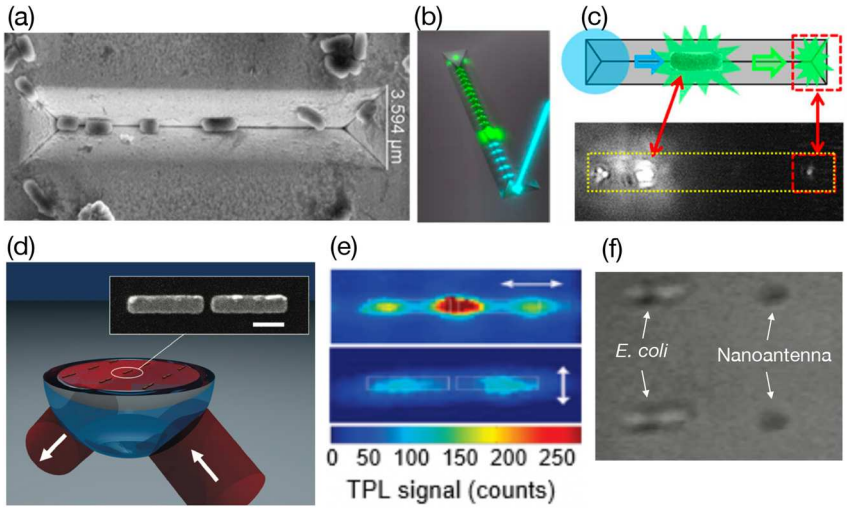

Figure 1: (a) Scanning Electron Microscope (SEM) micrograph of bacteria attached to a V-groove waveguide. (b, c) Fluorescence excitation and emission of bacterial guided in the groove [59]. (d) Schematic of a nanoantenna on a glass substrate and SEM micrograph of a single nanoantenna in the inset (scale bar: 200 nm). (e) Two-photon induced luminescence (TPL) from a single nanoantenna for both longitudinal and transversal polarization. (f) Optical trapping of two individual *Escherichia coli* bacteria on separate nanoantennas [61].

by a bacterium attaching to the surface, which is most sensitively realized via an interferometric readout. The first Mach–Zehnder interferometers were used to detect *L. monocytogenes* with a sensitivity of 10^5 CFU/mL [67]. Several improvements have since been made. For example, Maldonado et al. [68, 69] have demonstrated a bimodal waveguide for the detection of low concentrations of bacteria, that is, down to 40 CFU/mL. The device consists of an optical waveguide in Si_3N_4 supporting two modes with different polarization, as schematically shown in Figure 2(a). The advantage of this bimodal waveguide approach is that environmental fluctuations, especially temperature, affect both modes almost equally, which allows to improve the signal-to-noise ratio. A schematic and data taken with this technique are shown in Figure 2(b).

From a practical point of view, a limitation of the optical waveguide-based approach is the need to launch light into the waveguide, which requires rather demanding coupling arrangements and makes these devices not compatible with standard microscopes. As an alternative, the interferometer can be realized in an optical fibre, for which standardized coupling interfaces exist [70, 71]. The interferometer can be made of two identical chirped long period gratings (CLPGs) as illustrated in Figure 2(c). The first CLPG partially couples the light from the core mode to the cladding mode. Both modes propagate through the sensing area, where the fibre cladding is open and functionalized to detect attached bacteria. At the second CLPG, the cladding mode is coupled back into the fibre core, therefore interfering with the core mode. Because only the cladding mode interacts with the bacteria, their presence provides the phase shift and resulting interference signal. Figure 2(d) and (e) show how different concentrations of *E. coli* impact on the optical transmission spectra of the fibre. An LOD of only 7 CFU/mL of *E. coli* was reported [72], which highlights the remarkable sensitivity of this technique.

The major downside is that the tapered fibre is very fragile, which can lead to easy breakage. However, recent progress in judicious packaging has enabled nanostructured fibres to be used directly in tissue for the detection of cancer biomarkers [73] or in ready-to-eat meat for the detection of pathogenic bacteria [74]. These results highlight the importance of fibre sensors and demonstrate the opportunity for the *in vivo* detection of bacteria. Finally, it is interesting to note that interferometric waveguide sensors, which are extremely sensitive for protein sensing, do not perform as well as resonant ones for the detection of individual bacteria. The reason lies in their *modus operandi* because an interferometric sensor derives its sensitivity from the long interaction length and the assumption that the sensing arm is uniformly covered by the measurand. Even though low concentrations of bacteria have been detected, an interferometric waveguide does not allow for bacteria localization. Therefore, if the goal is to monitor individual or small numbers of bacteria, then the long interaction length offers no advantage and a resonant modality is preferable. This modality is discussed in the next section.

2.2.2 Resonant metasurfaces

Resonant metasurfaces use nanostructures to create distributed resonances for specific wavelengths

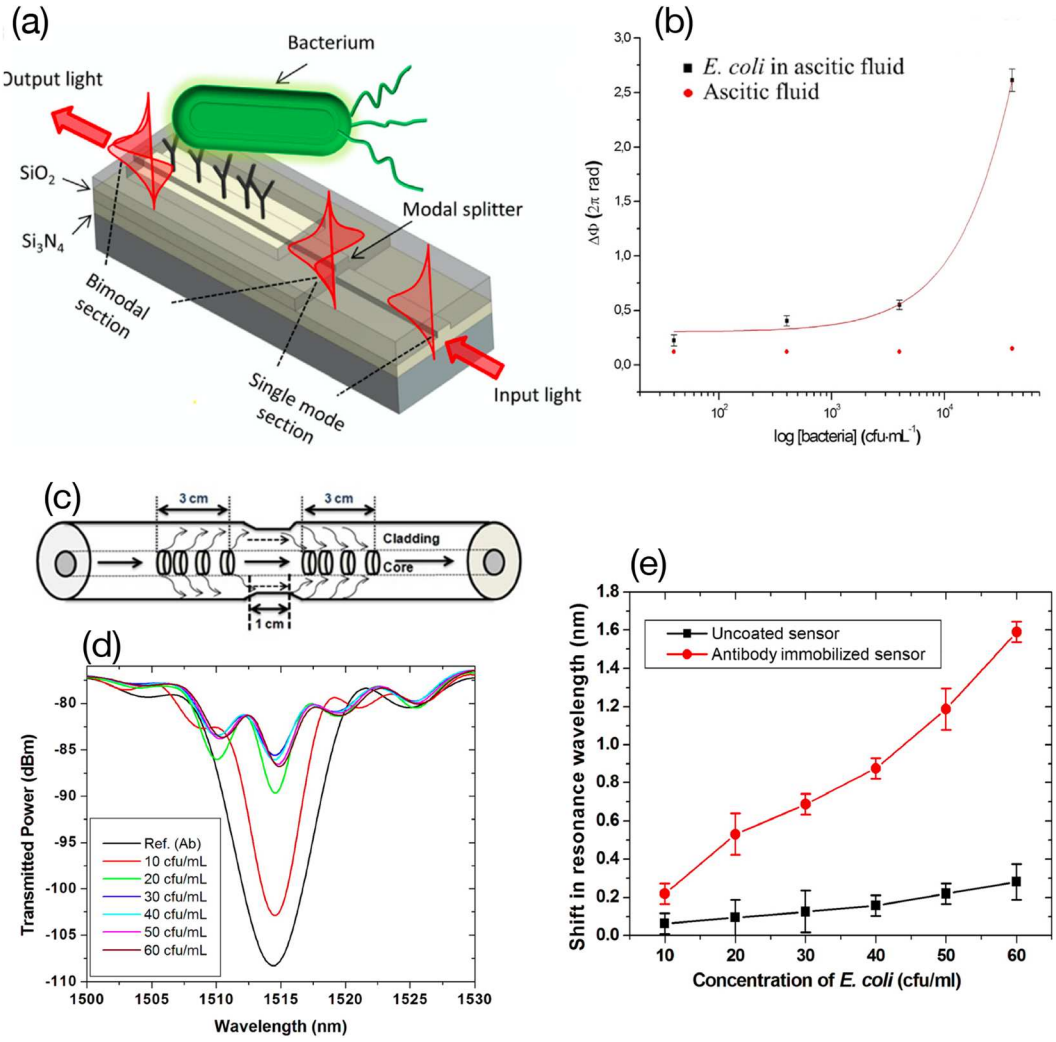

Figure 2: (a) Schematic of the dielectric bimodal waveguide (BiMW) (left) and (b) measured phase change versus *Escherichia coli* concentration [68]. (c) Schematic of the cascaded chirped long period grating inscribed in the fibre core with (d) corresponding transmission spectra for different concentrations of *E. coli*. (e) Wavelength shift of the functionalised (red line) and bare (black line) sensor with exposed to *E. coli* concentrations from 10 to 60 CFU/mL [70].

determined by their period, thickness and/or fill-factor. These resonant structures sample the bacterium multiple times, so they can be understood as multipass devices, whereas interferometric waveguides are single-pass devices. The multipass nature of the resonant structure provides high sensitivity, while also affording out-of-plane coupling, which simplifies optical characterization.

Despite the resonant enhancement and simplicity of optical interrogation, initial reports did not achieve the sensing or imaging of single cells. In fact, most of these sensors have been limited to the quantification of bacterial concentrations, with typical LODs of ~200 CFU/mL obtained for *Legionella neumophila* with a polymer 2D PhC [75]. Different approaches have been used to improve resolution. In particular, the combination of 2D photonic crystals (PhCs) with hydrogels [76, 77] has improved the resolution down to 32 CFU/mL of *E. coli* [77], although a number of complex preparation steps are required to achieve this result. An alternative way to improve the LOD is by using the field enhancement offered by PhCs to enhance fluorescence. For instance, a polymeric 2D PhC was used to detect the fluorescence of resorufin, a compound often used as a proxy of bacterial presence and viability. Even though this method is not label-free, an LOD of 10 CFU/mL of *E. coli* was demonstrated in wash water [78].

More recently, we have introduced a label-free resonant metasurface based on a nanohole array in amorphous silicon (a:Si) that exhibits Fano resonances with a dynamic range from near 0% to near 100% reflection and a *Q*-factor of 300–400 [32]. Surprisingly, these high-*Q* resonances also

exhibit a very high spatial resolution, that is of order 1 µm or better, when used for hyperspectral imaging. This capability is illustrated in Figure 3, where we use the combination of strong localization, high Q factor and high dynamic range of the optical mode to provide a quantitative analysis of the refractive index distribution and imaging of a single *E. coli* cell. These results clearly demonstrate that the metasurface approach can be used for nanoscopic analysis because the refractive index being probed is that of the bacterial membrane. This ability could open up a variety of studies including, for example, cell adhesion and secretion monitoring that have previously only been demonstrated with mammalian cells [79, 80], but have never been applied to bacteria. Monitoring the response of bacteria to antibiotic challenge is another promising area of research opened up by these structures, which is discussed in more detail in Section 3.

2.2.3 Dielectric nanotweezers

Dielectric nanotweezers are of particular interest because they can enhance near-field forces while minimizing the thermal effects typical of plasmonic configurations because thermal effects have been shown to be detrimental to trapping stability [81, 82]. For example, the trapping of DNA molecules was demonstrated in a slotted waveguide [83] and nanotweezers based on dielectric waveguides are already available commercially as portable instruments (OPTOFLUIDICS, Inc). The main limitation of nanophotonic waveguides is their lower field enhancement compared with metallic nanostructures, which means that typically higher powers are required to achieve trapping. However, the trapping of bacteria is somewhat easier because of their volume, and the optical manipulation of bacteria with silicon waveguides has been successfully demonstrated with relatively low power (100 mW source power, corresponding to a few milliwatts coupled into the waveguides) [84].

An interesting configuration has been recently proposed by Zhao et al. [85], who fabricated waveguide pairs separated by gaps of 200 nm. The small gap allows light to be coupled laterally back and forth between the two waveguides, therefore creating numerous trapping spots and effectively generating an optical lattice. By using a guided power of 3 mW, the authors managed to trap and align individual *Shigella* at a rate of 12 bacteria/min and conduct single-cell viability studies on exposure of the trapped bacteria to ethanol.

Moving from one-dimensional confinement in waveguides to two-dimensional confinement in cavities allows increasing the resonant enhancement further. The stronger light-matter interaction provided by a two-dimensional resonator leads to higher optical forces and therefore a reduction in the input power needed. In addition, the self-induced back-action mechanism can be exploited, which enhances the restoring force that draws the bacterium back into the trapping site when it tries to escape. This mechanism is the main reason for the stable trapping that has been achieved with very low optical power, that is orders of magnitude lower than the power needed for conventional bulk trapping [86]. For example, van Leest and Caro [87] achieved stable trapping of individual bacteria with PhC cavities requiring only 400 µW for both Gram-negative (*E. coli*) and Gram-positive (*Bacillus subtilis*) bacteria.

Other examples include photonic crystal nanobeam cavity and hollow PhC configurations [21, 22] that have shown not only to trap, but also to analyse single bacteria on chip. In particular, the stable trapping of individual *E. coli*, *Staphylococcus epidermidis diplococcus* and *B. subtilis* was observed using only hundreds of microwatts of (estimated) power in the cavity. Both types of cavities allowed distinguishing bacteria by size, shape and motility patterns via the magnitude of the observed change in the transmission spectrum of the cavity and the noise of the transmission trace. A further improvement was achieved with the 2D side-coupled PhC cavity shown in Figure 4(a), whereby a statistical analysis of the transmitted optical power enabled the authors to correctly differentiate between Gram-positive and Gram-negative bacteria within a

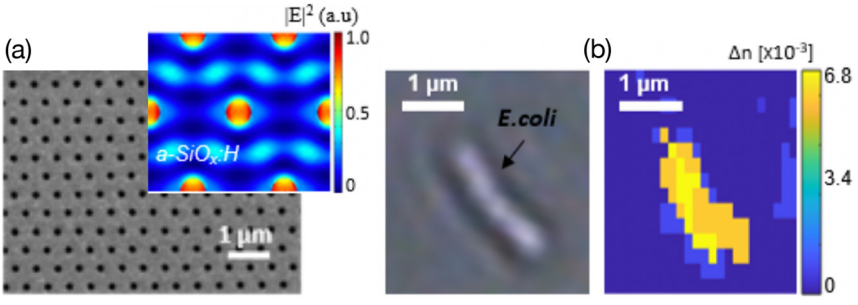

Figure 3: (a) Scanning Electron Microscope (SEM) image of the dielectric nanohole array and simulated electric field at resonance in the inset. (b) Brightfield microscope versus hyperspectral images of an individual *Escherichia coli* obtained with a dielectric nanohole array [32].

few seconds [22]. Typical histograms of the relative transmission are shown in Figure 4(b).

Being able to extract so much information is clearly enabled by the strong overlap of the bacterial cell wall with the evanescent field of the cavity mode. In fact, Therisod et al. [22] were able to use the histograms in Figure 4(b) to explain the intrinsic heterogeneity of the bacterial phenotype as well as the differences in the composition of the bacterial membrane of different species. For instance, the authors noted that Gram-negative bacteria consistently induced a larger change in transmission compared with Gram-positive species. This observation correlates well with the larger deformability of the cell wall of Gram-negative species, as well as with the presence of lipopolysaccharides molecules exclusive to the cell wall of Gram-negative bacteria. Importantly, the size of the bacteria is not the main discriminator in Figure 4(b) because the length of both Gram-stain bacteria ranges between 0.5 and 4 μm.

From the aforementioned, it is clear that optical trapping can provide significant information on the morphology and the motility of bacteria. Recently, we have proposed to add another dimension to this toolkit by investigating the possibility of conducting electrical impedance measurements on optically trapped bacteria. The idea builds on the "electrophotonics" principle we introduced earlier, whereby the judicious doping of silicon allows conducting electrochemical measurements on the surface of an optical waveguide structure in a high-Q silicon microring resonator [88, 89]. Using similar principles, we considered an arrangement that combines silicon photonic crystal cavities for optical trapping with doped regions for conducting impedance measurements [90]. A schematic of a single trap is shown in Figure 4(c). The idea is to monitor changes in morphology and motility optically, as previously mentioned, together with changes in impedance as the trapped bacterium is challenged by various antibiotics (Figure 4(d)). We expect that such a multiparametric approach will provide a more accurate and potentially faster susceptibility analysis [25], while placing multiple such nanotweezers into an array allows probing multiple bacteria in parallel and can therefore also provide information on population heterogeneity.

An alternative waveguide geometry is to use an optical fibre for trapping. This is clearly not nanoscopic, as the fibre achieves trapping through a focussed Gaussian beam created by tapering or lens-ending the fibre but is much more versatile than a focussed beam created by a microscope lens. For example, Xin et al. [91] demonstrated the trapping of a single *E. coli* by fabricating a nano-tip on the end of a single-mode fibre. The fibre is also tapered to focus the light away from the tip while creating a sufficiently strong energy confinement (Figure 4(e)) to ensure that the bacterium is localized in all three dimensions. Examples of a trapped *E. coli* are shown in Figure 4(f). This approach offers interesting opportunities for bacterial studies as it enables probing bacterial motility and dynamics in different environments, possibly even *in vivo*.

However, the main limitation of fibre-based tweezers is their weak optical gradient compared to integrated nanotweezers, which means that higher optical powers are required to achieve stable trapping. For example, a power of about 50 mW, corresponding to a power density of ~10^{10} W/m^2 (or 50 mW/μm^2), was needed to trap a single *E. coli* bacterium in the experiments by Xin et al. [91]. The experiment only achieved stable trapping for approximately 2 min, whereas many studies require longer observation times (Table 2). A more stable trap may require higher power, which may then become phototoxic [63].

3 Photonic techniques for antimicrobial susceptibility testing

To help appreciate the advantages of photonic techniques for susceptibility testing (AST), we start by briefly introducing the traditional microbiological ASTs, which belong to the macroscopic category of techniques. We then move onto microscopic free-space optics techniques which afford measuring fewer bacteria, but still probe whole cells. Finally, we discuss nanoscopic devices based on guided-wave optics which limit light-matter interaction to the bacterial membrane. We also briefly describe some light-based instruments that have already been successfully commercialized. Throughout this entire section, it is important to remember that ASTs begin with an isolation step, which serves to isolate the bacteria of interest from a complex biological sample, such as urine or blood. This procedure requires culturing and, therefore, at least an overnight incubation on agar plates [93, 94]. After the isolate is obtained, the actual AST is carried out by exposing bacteria to certain antibiotics. In this respect, all the times to result mentioned in this section (and reported as "drug test time" in Table 3) only refer to the drug testing procedure, as most of the current ASTs techniques require a pure bacterial isolate as a starting point [4, 95].

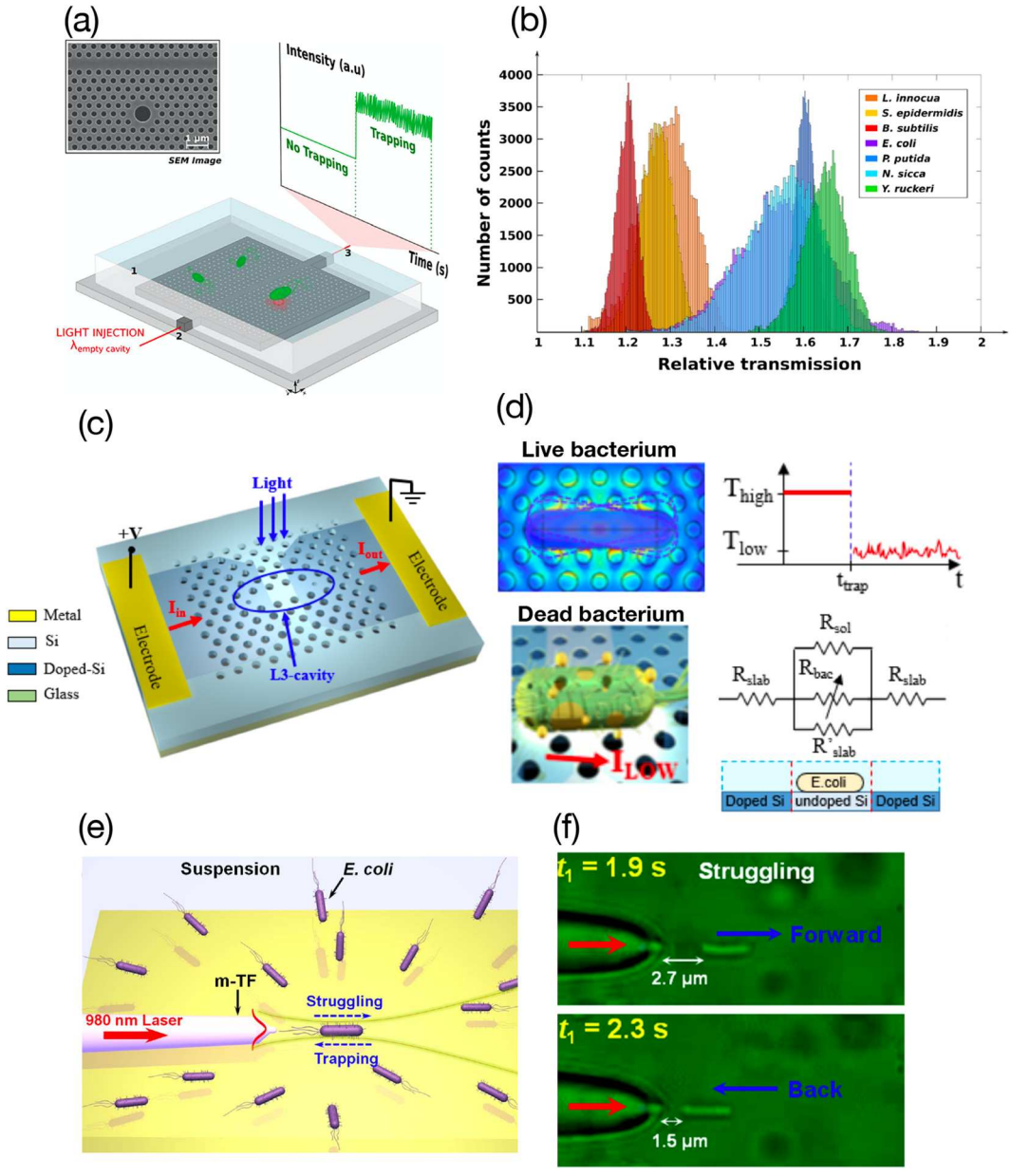

Figure 4: (a) Illustration of the 2D PhC hollow cavity and Scanning Electron Microscope (SEM) image used for trapping individual *Escherichia coli* by Therisod et al. [22]. (b) Histograms of the relative transmission measured for seven different bacteria. (c) Schematic of an electrophotonic trap simulated by Conteduca et al. [90]. (d) Optical and electrical detection principles of individual bacteria. (e) Schematic of the lensed fibre for contactless trapping of individual *E. coli*. (f) Trapping of individual *E. coli* achieved with the nanostructured fibre [91].

3.1 Traditional microbiological techniques

The traditional method for assessing antibiotic susceptibility is the disk diffusion test developed in the 60s by Bauer and Kirby [96], a schematic of which is shown in Figure 5(a). On overnight incubation of bacteria on an agar plate, the size of the clear rings surrounding antibiotic-impregnated filter-paper disks are used to inform antibiotic efficacy in stopping bacterial growth. Although this technique is easy to perform and inexpensive, it suffers from slowness (24–48 h) and from being only semi-quantitative, so that the lowest concentration of antibiotic that inhibits bacterial growth (the minimum inhibitory concentration, MIC) can usually not be determined.

A more robust solution is provided by microdilution assays [97], whereby bacterial inoculums are added to micro-wells and incubated overnight with two-fold dilutions of antibiotics, as shown in Figure 5(b). Bacterial growth is then quantified by measuring the OD of the suspension. A clear suspension corresponds to a low OD

Table 1: State of the art of nanophotonic sensors for bacteria detection and imaging.

Configuration	Application	Resolution[a]	Solution	Time[b]	Reference
SPR with polymeric film	Detection	0.57 CFU/mL *E. coli*	Buffer	20 min	[37]
Plasmonic nanohole array	Detection	1 CFU in 10 µL *E. coli*	Urine	15 min	[42]
Plasmonic nanohole array with interferometry	Detection	1 CFU in 10 µL *E. coli*	Diluted plasma	40 min	[31]
Dielectric BiMW	Detection	12 CFU/mL *B. cereus* 4 CFU/mL *E. coli*	Buffer Ascetic fluid	12 min 25 min	[68, 69]
Hydrogel 2D PhC	Detection	58 CFU/mL *E. coli*	Milk, orange juice, river water, serum	6–12 min	[76]
Chirped long period fibre	Detection	7 CFU/mL *E. coli*	Buffer	12 min	[70]
SPR	Imaging	1 CFU *Listeria*	Tryptic Soy Broth (TSB)	<7 h	[46]
Dielectric nanohole array metasurface	Imaging	1 CFU *E. coli*	Buffer	<30 min	[32]

[a]The resolution is reported in CFU/mL when the aim is only to quantify bacterial concentration and in absolute number of bacteria when the sensor localizes bacteria for imaging. [b]The detection time reported is not intrinsic to the photonic techniques, but it is also affected the surface functionalization protocol used to tether bacteria onto the sensors' surface.

Table 2: State of the art of photonic nanotweezers for single bacterium trapping.

Configuration	Power	Trapping time	Application	Reference
V-groove plasmonic waveguide	/	/	*E. coli* detection by fluorescence signal	[59]
Plasmonic nanoantenna	100 µW/µm^2	>2 h	Trapping and growth monitoring of multiple individual *E. coli*	[61]
Dielectric 2D PhC (H0, H1, L3 cavities)	400 µW	>5 min	Trapping of *E. coli* and *B. subtilis*	[87]
Dielectric 1D PhC (nanobeam cavity)	~100 µW	10 min, >1 h, >1 h	Single *B. subtilis*, *E. coli*, *S. epidermidis*	[92]
Dielectric 2D PhC (side-coupled hollow cavity)	~100 µW	Several minutes	Differentiation between Gram-positive and Gram-negative bacteria	[22]
Lensed optical fibre	50 mW	2 min	Dynamic observation of single *E. coli*	[91]

and is indicative of little or no growth, hence antibiotic effectiveness, as shown schematically in Figure 1(c). Although these techniques are commonly used in clinical settings and microbiology laboratories, they have a long turnaround time because of the need for overnight incubation. In addition, they require specialized personnel because of the labour-intensive procedures of plating, diluting reagents and preparing trays.

3.2 Commercial devices

The problem of ease of operation has been partly addressed by commercial instruments, such as VITEK2 [98] (BioMérieux), MicroScan WalkAway [99] (Siemens Healthcare Diagnostic) or BD Phoenix [100, 101] (BD Diagnostics). Most of these instruments are based on a photonic readout of OD or fluorescence of bacterial cultures in microwells as indicators of bacterial growth and/or metabolism in the presence of antibiotics.

These instruments introduced desirable features such as automation of sample loading and processing as well as a multiplexing capability; the VITEK2, for example, can perform up to 240 tests simultaneously. In terms of time to result, these instruments are capable of generating results in 3.5–16 h (see Table 3), thereby representing some improvement compared with the more traditional techniques [98, 102, 103]. The improvement is limited, however, because the detection is fundamentally culture-based. Furthermore, these techniques also neglect heterogeneity by averaging over the entire bacterial population. Finally, it is important to note that significant discrepancies between the results obtained with these instruments, and with the traditional methods have been reported. For these reasons, it is difficult to define a true "gold standard" for a susceptibility test [104–107].

Table 3: Overview of photonic antimicrobial susceptibility tests in comparison with traditional microbiological and commercial solutions.

Class	Methods	Structure	Detection principle	Susceptibility indicator(s)	Surface receptors/ labels	Drug test time*	Probed bacteria	Sample nature and volume	Reference
Traditional culture-based (macroscopic)		Disk diffusion (Kirby-Bauer)	Visual inspection	Growth	None	16–24 h	Bulk method	Isolates on MH agar	[96]
		(Micro)broth dilution	Colorimetric or OD reading	Growth or metabolism	None	16–24 h	Bulk method	Isolates in MH broth (100 µL/ well)	[97]
Free-space optics (microscopic photonics)	Commercial devices	VITEK2 (BioMérieux)	OD and/or fluorescence measurements	Growth, metabolism	None	3–15 h	Bulk method	Isolates in saline (3 mL)	[98, 102, 103]
		MicroScan Walkway	OD and/or fluorescence measurements	Growth	Fluorophores	4–16 h	Bulk method	Isolates in saline (30 mL)	[99]
		BD Phoenix	OD and colorimetric reading	Growth, metabolism	Chromophores	6–16 h	Bulk method	Isolates in Phoenix AST-S broth (4.5 mL)	[100, 101]
	Forward laser light scattering	BacterioScan®	Small-angle scattered light	Growth, morphology	None	2–6 h	$>10^4$ CFU/ mL	Isolate in saline/ urine (2 mL/ well)	[26,110–112]
	Flow cytometry	Commercial flow cytometers	Transmitted and/or scattered light and/or fluorescence	Cell count, morphology, membrane integrity	Fluorophores (optional)	1.5–6 h	1	Isolates in MH (6 mL) Spiked blood (0.5 mL)	[114, 115]
	Nanostructure-enhanced detection	Silicon nanopillars	Optical interference	Growth	Wheat germ agglutinin (WGA)	2–3 h	$>10^3$ CFU/ mL	Isolate in PBS (500 µL)	[121]
		2D nanodisks grating	Optical diffraction	Growth, motility, diffusivity	None	2–3 h	>1–5	Isolate in LB broth (150 µL)	[118]
Guided-wave optics (nanoscopic photonics)	Evanescent-wave sensors	Gold thin film SPR	SPR resonance angle	Membrane integrity	Poly-L-lysine	0.5–3 h	Not given	Isolate in LB broth (not given)	[23]
		Gold nanoholes	Extraordinary optical transmission	Growth	Anti–*E. coli* antibodies	2 h	$>10^2$ CFU/ mL	Isolate in PBS (1 mL)	[122]
		Gold nano-mushrooms	LSPR resonance wavelength	Growth	Conditioning layer	2 h	Not relevant	Isolate in LB broth (125 µL)	[125]
		Si_3N_4 1D grating	GMR resonance wavelength	Growth	None	5 h	Not relevant	Isolate in LB broth (40 mL)	[128]
		Gold thin film SPR	SPR imaging	Nanomotion	Anti–*E. coli*/APTES	<1 h	1	Isolate in PBS (20 µL)	[51]

*The drug test time refers to the time needed to identify susceptibility in a pure bacterial colony, therefore does not include pre-culturing time for either sample isolation or enrichment (typically at least overnight).

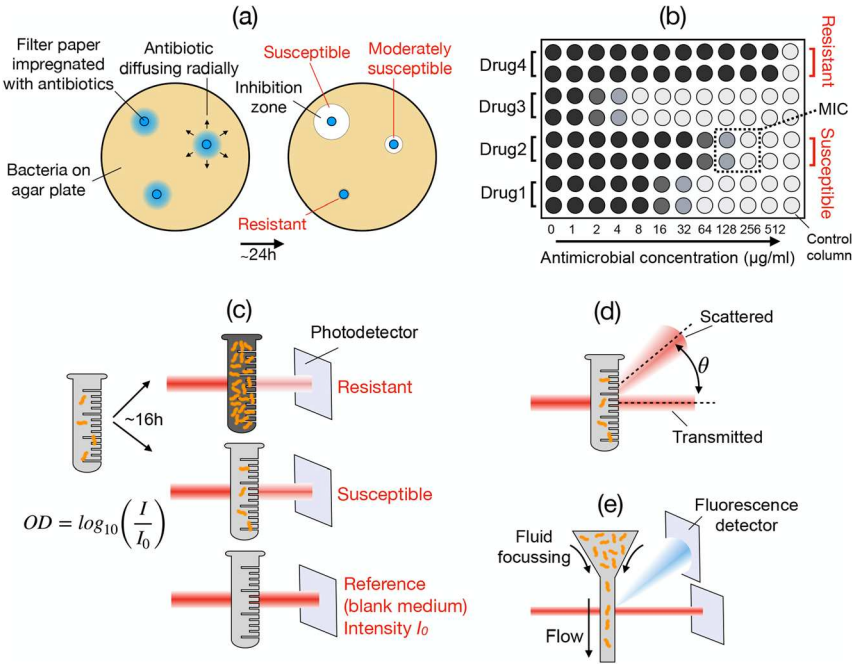

Figure 5: (a) Schematic illustration of the Kirby-Bauer disk-diffusion antimicrobial susceptibility test. Bacterial colonies are spread uniformly onto an agar plate and their susceptibility is determined by the size of the inhibition zones surrounding the antibiotic-impregnated disks. (b) Schematic of a microdilution assay, where bacteria are exposed to serial dilution of different drugs. Dark wells are indicative of viable bacteria that have managed to duplicate, whereas clear ones indicate that bacteria did not grow. (c) Optical density (OD) measurement scheme. A turbid solution contains higher concentrations of bacteria, therefore absorb more light. (d) Schematic of light scattering techniques, whereby light transmitted and scattered by the bacterial sample are both measured. (e) Flow cytometry working principle. Single bacteria are flown across a laser beam to detect both the transmitted light and emitted fluorescence from single bacteria.

3.3 Free-space photonic techniques

3.3.1 Elastic light scattering

A more refined version of microdilution is the use of elastic light scattering. While microdilution simply measures the light absorbed by a growing bacterial culture, light-scattering also analyses the angular intensity spectrum of the light scattered by the bacterial sample, as schematically illustrated in Figure 5(d). The angular spectrum carries two pieces of information: its intensity is proportional to the number of scatterers, that is the bacterial count, hence is a proxy for bacterial growth, whereas the shape of the spectrum depends on the size and morphology distribution and of the scatterers. These ideas were applied to antibiotic testing as early as the 1970s, when Berkman et al. [108] and Murray et al. [109] observed significant differences in the light scattered by antibiotic-treated versus untreated samples. The technology has been improved since and has recently been commercialized as the BacterioScan® instrument [26], which is especially designed to analyse urine samples and related urinary tract infections. The instrument measures the forward laser light scatter (FLLS), that is the laser intensity scattered by the bacterial sample at small angles compared with the incident direction and can measure OD values 1 to 2 orders of magnitude lower than traditional laser absorbance techniques. Consequently, it can detect bacterial growth from a much earlier stage, affording time to result of 2–6 h in urine [110–112] and even in blood samples [113]. Notably, the device can perform 16 tests simultaneously.

Even though FLLS affords parallel, multiplexed and relatively fast measurements, it still struggles with concentrations lower than 10^4 CFU/mL (see Table 3). In particular, BacterioScan is not suitable for single, or few, bacteria measurements, such that the heterogeneity of bacterial colonies is still disregarded. Another limitation is that the optical probing volume is determined by an unfocussed laser beam, hence macroscopic, and background noise may interfere with the measurement.

3.3.2 Flow cytometry

A further application exploiting laser-light interaction with bacteria is represented by flow cytometry, where the key idea is to rapidly flow cells across a detection area illuminated by a fixed light beam. Critically, the bacterial suspension is hydrodynamically focussed through a nozzle, so that individual cells pass through the laser beam, as illustrated in the schematic in Figure 5(e). Therefore, flow cytometry restricts the interaction of light to individual cells without the need for light structuring or confinement. Both the transmitted/scattered light and possibly their fluorescence, if the cells are specifically tagged, are detected. The scattered light enables counting cells and analysing their size and morphology, while fluorescent labelling can inform the presence of specific proteins or markers. By choosing appropriate fluorophores, one can probe the mechanical

integrity of the bacterial membrane and its functionality (such as the membrane potential) as well as bacterial viability. Thanks to this richness of information, flow cytometry has been successfully used for AST, both with and without fluorescent tagging, with time to result of 1.5–8 h [114–116].

The main advantages of flow cytometry are rapid assay times and single-cell capability with high-throughput. However, although tens of thousands of cells per second can be flown through the laser beam and analysed, the technique is rather demanding in terms of detection equipment. Fast and sensitive detectors are required to excite and reveal fluorescence at a frequency of up to 10 kHz. In addition, certain bacterial strains emit autofluorescence, hence causing false positive/negative and increasing noise [117].

3.3.3 Nanostructure-enhanced detection

The free-space photonic structures examined thus far do not exploit any nanostructure to shape or interact with light. We now consider approaches that use nanostructures to generate interferometric or diffractive effects and examine whether advantages can be gained from these structures for the assessment of bacteria. Importantly, field enhancement does not play a role in the particular structures examined in this section as they do not confine light. Instead, nanostructuring is used to generate interference and diffraction which increase sensitivity to bacterial growth so that rapid ASTs can be performed.

For example, Volbers et al. [118] exploited the diffraction generated by a grating made of a 2D array of gold nanodisks. The intensity of the first-order diffraction mode is recorded by a CMOS camera placed at an appropriate angle, as seen in Figure 6(a). Bacteria growing onto or above the grating surface (see the Scanning Electron Microscope (SEM) picture in the inset of Figure 6(a)), disturb the diffraction because they act as additional scattering centres. As a result, the decrease and fluctuations of intensity in the diffracted mode are monitored and linked to the number of bacteria and their motility, respectively. Figure 6(b) shows how the decrease of diffraction intensity depends to the number of bacteria. Notably, the system is sufficiently sensitive to pick up the presence of a few (1–5) bacteria within the observed grating area of $(120 \times 120)\ \mu m^2$.

The system was then used to determine the MIC of several bacterial strains exposed to three different antibiotics and susceptibility was demonstrated within 2–3 h. Figure 6(c) shows the case of ampicillin by plotting the change in diffracted mode intensity over time and for different concentrations of the drug. The constant intensity over time observed for concentrations of ampicillin higher than 2 mg/mL is indicative of no growth, and therefore drug efficacy. Interestingly, the fluctuations in intensity are shown to be an even earlier predictor of susceptibility than intensity alone, pointing to motility as an early indicator of susceptibility. For example, the action of ampicillin was detected in 20–30 min as a significant decrease of the normalized standard deviation of the intensity traces, as illustrated in Figure 6(d) for a susceptible *E. coli* strain, as opposed to the 1.5–2 h required for distinguishing the intensity curves in Figure 6(c). Conversely, the signal collected from resistant bacteria shows continuously increasing fluctuations due to the increasing number of bacteria contributing to the signal (see Figure 6(e)).

This observation is in agreement with the study of fluctuations conducted on other platforms, such as hydrodynamic trapping of individual bacteria or the electrical fluctuations induced by a few tens of bacteria in a microfluidic channel [25, 119]. Similarly, monitoring the nanomotion of bacteria tethered to AFM cantilevers produced compatible results in terms of detection time [24, 120]. Overall, these findings suggest that measuring bacterial fluctuations, which are proportional to bacterial motility, is a more powerful and earlier indicator of viability than growth, so is worth exploring further as a reporter of susceptibility to antibiotics. A further advantage of the nanodisk configuration is that no surface receptors are required because the bacteria do not need to be in direct contact with the surface to disturb the diffraction.

We note that other macroscopic and free-space techniques are not able to record the motility of a few bacteria either because they average over a much larger number of bacteria or they only obtain temporary information (such as flow cytometry). Conversely, the nanodisk are much more sensitive, such that they can record as few as 1–5 bacteria (see Figure 6(b)), therefore allowing for both bacterial division and fluctuations to be monitored from an early stage.

Another example that utilizes nanostructures to create Fabry-Pérot resonances was proposed by Leonard et al. [121]. Their sensor is based on a silicon micropillar array with a functionalized surface to bind bacteria, as shown in the SEM picture in Figure 6(f). The micropillar array generates Fabry-Pérot fringes in the vertical direction, with interference happening between the portion of the beam reflected off the top of pillars and the one reflected off the bottom. The presence of bacteria modifies the refractive index between the pillars and, consequently, the optical phase, resulting in a shift of the fringes (see Figure 6(g)).

Bacteria were grown on the array and the shift of the fringes was monitored over time as a proxy of bacterial

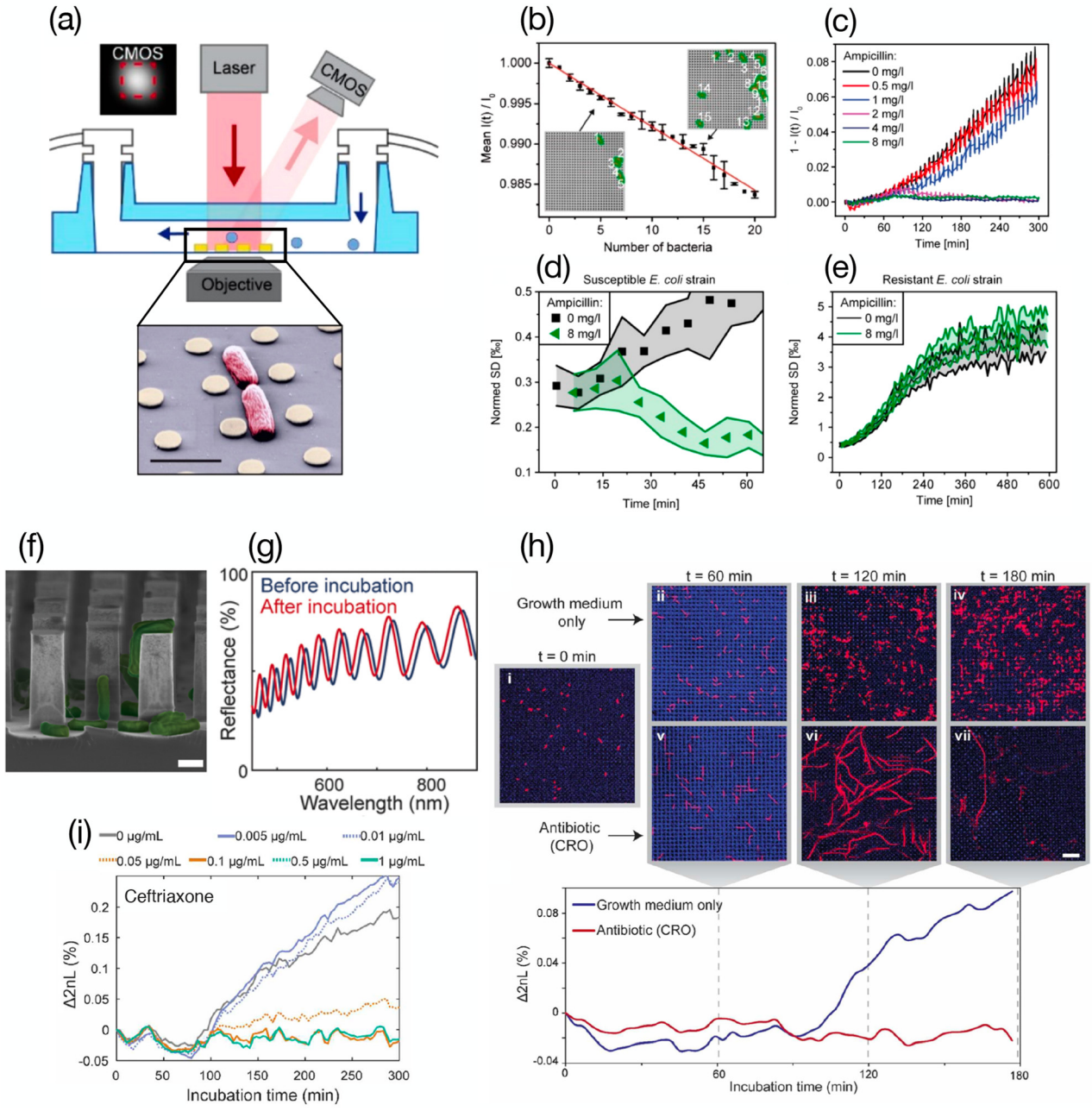

Figure 6: (a) Schematic of the measurement setup used by Volbers et al. [118]. The inset shows a false-colour Scanning Electron Microscope (SEM) image of the nanodisk array and a single *Escherichia coli*. Scale bar: 2 µm. (b) Mean decrease in diffraction intensity as a function of the number of bacteria above the grating. (c) Change of diffraction intensity in the presence of different concentrations of ampicillin. (d–e) Normalized change of standard deviation of the intensity fluctuations for susceptible and resistant *E. coli* in the presence of 8 mg/mL of ampicillin. (f) False-colour SEM picture of *E. coli* situated between the silicon micropillars fabricated by Leonard et al. [121]. Scale bar: 1 µm. (g) Interference fringes measured on illumination of the micropillar array. (h) Fluorescent images and percentage change of optical path difference as a function of time for *E. coli* growing over the micropillar in clear growing medium and ceftriaxone. Scale bar: 10 µm. (i) Percentage change of optical path difference over time for different concentrations of ceftriaxone.

growth. As Figure 6(h) shows, the signal behaves differently when the antibiotic ceftriaxone is added to the bacterial culture compared with a control experiment without antibiotic. Specifically, no increase in signal is observed when bacterial growth is inhibited (red curve), as opposed to the no-drug case, where growth occurs instead (blue curve). The different growth conditions were verified with fluorescent images as shown in the top row of Figure 6(h). The technique

was also able to measure MIC values. For example, Figure 6(i) shows that for concentrations of ceftriaxone greater than 0.01 μg/mL, no change in phase is observed over time. Conversely, for lower concentrations of antibiotics, a significant increase is observed, hence allowing an MIC value to be determined within 2–3 h of monitoring.

In this case, the enhanced light-bacteria interaction offered by the Fabry-Pérot resonance affords higher sensitivity compared with traditional free-space interaction or OD measurement. Even though bacterial growth is still being used as a signature, here the bacterial optical mass is being picked up interferometrically, which in general affords higher sensitivity. Although the principle of phase-based detection has been widely used in biosensing, it has not been as much exploited for bacterial drug testing, therefore representing an interesting opportunity for future developments. In fact, exploiting optical interference enabled a reduction of detection time from 2–16 h, typical for free-space methods, to 2–3 h, as summarized in Table 3.

3.4 Evanescent wave-based ASTs

In contrast to the free-space techniques described previously, evanescent-wave sensors are based on guided modes and resonances and they interact with the analyte via their evanescent tail. The confinement of the evanescent tail to within a few hundreds of nanometres from the interface classifies these devices as surface sensors and implies that only the cell wall of the first layer of bacteria is probed, as described in the introduction and underpinned by equation (1). We therefore classify these techniques as nanoscopic, as indicated in Table 3, in contrast to microscopic techniques that instead probe the entire cell. Interestingly, some of the techniques are only nanoscopic in one dimension, that is they probe the bacterium within a few hundred nanometres of the surface but average over an illuminated area of 100s of μm or even millimetres, whereas others are much more localized and are able to probe individual bacteria. SPRi or hyperspectral imaging with GMRs [20, 49, 79], fall into the latter category.

Regarding sensors that probe a larger area, one of the first examples was reported by Chiang et al. [23], who used an SPR sensor functionalized with poly-L-lysine to encourage bacterial adhesion and made two important observations. First, bacteria susceptible to ampicillin showed a reduction of refractive index compared with resistant bacteria on exposure to ampicillin. This indicates attack of the cell membrane and is consistent with the fact that ampicillin inhibits bacterial cell wall synthesis (see the light-grey curve in Figure 7(a)). Second, the sensor can discriminate between the actions of different drugs. Tetracycline, for example, binds to the bacterial ribosomes and inhibits protein synthesis, but does not affect the cell wall. Correspondingly, very little reduction in refractive index was observed after the administration of the antibiotic. Instead, the inhibition of protein synthesis causes delayed and irregular fluctuations in the SPR angle as a distinct signature (see the dark-grey curve in Figure 7(a)).

Importantly, these changes are measured on a short timescale because of the surface sensitivity; the evanescent tail of the mode is able to directly interact with the bacterial membrane and to monitor any changes instantaneously. Therefore, the process is limited by the biological timescale of the drug's action and not by the sensitivity of the measurement.

Similarly, the high surface sensitivity of the confined optical mode can also be used to monitor bacterial growth directly and on a much shorter timescale than traditional growth assays. This effect was exploited by Kee et al. [122] who functionalized the surface of a gold nanohole array with antibodies to monitor the growth of tethered *E. coli*. Figure 7(b) displays a sketch of the structure and an SEM image of a fabricated array, whereas Figure 7(c) shows the wavelength shift induced by bacteria growing on the sensor's surface. Because the bacteria were resistant to ampicillin but susceptible to tetracycline, a different behaviour was observed on exposure to the two drugs. In the presence of ampicillin, bacteria kept attaching and growing, hence increasing surface coverage over time and resulting in a continuous increase of the wavelength shift (blue curve). Conversely, tetracycline inhibited bacterial growth, which is evidenced by the immediate flattening of the curve after the addition of antibiotics (red curve).

As another example, the strong light confinement offered by localized surface plasmon resonances (LSPRs) on nanoparticles has been applied to speed up susceptibility testing of bacterial biofilms compared with traditional techniques. LSPRs are collective oscillations of free electrons induced by light in subwavelength metallic nanoparticles. On resonance, the electric field at the surface of the nanoparticle is strongly enhanced and decays with a short distance (tens of nanometre), thereby enabling evanescent-wave optical sensing [123, 124]. Funari et al. [125] fabricated gold nanoparticles supported by silica pillars, as shown in the sketch in Figure 7(d) and imaged in Figure 7(e). These structures, dubbed gold nanomushrooms, support a broad ($Q \lesssim 10$) LSPR mode which was used to monitor an *E. coli* biofilm forming over the surface in the presence of different antibiotics.

By measuring the wavelength shift of the LSPR mode, the authors showed that biofilm formation is only party hindered by drugs that target the bacterial adhesion

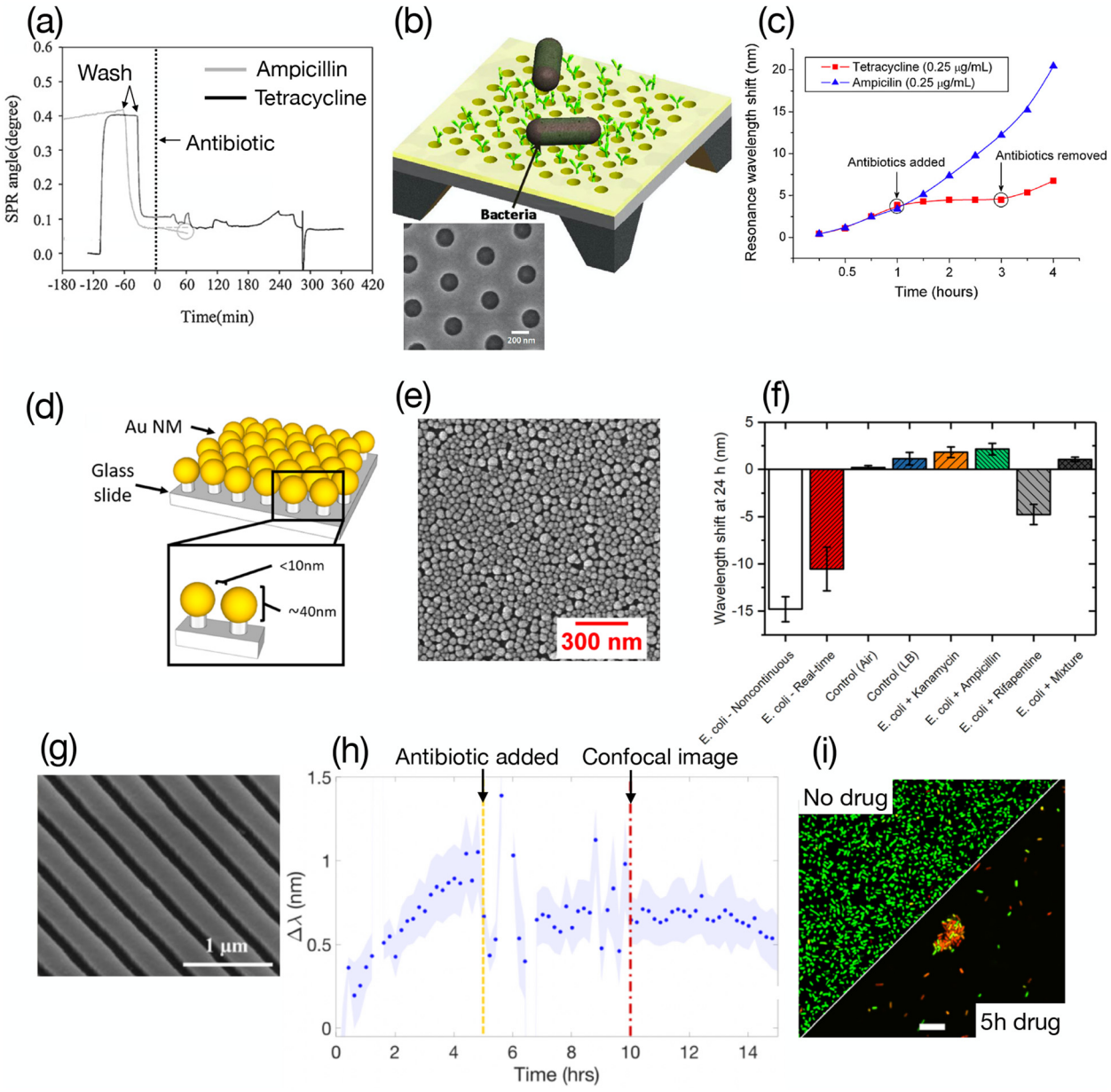

Figure 7: (a) Shift of surface plasmon resonance (SPR) angle induced by exposing susceptible *Escherichia coli* tethered on the SPR sensor to ampicillin and tetracycline [26]. (b) Sketch of the gold nanoholes used by Kee et al. and Scanning Electron Microscope (SEM) image of a fabricated array [122]. Scale bar: 200 nm. (c) Resonance wavelength shift for ampicillin resistant and tetracycline susceptible in the presence of ampicillin (blue curve) and tetracycline (red curve). (d) Gold nanomushroom array proposed by Funari et al. [125], (e) SEM image of the nanomushroom sensor's surface. (f) Wavelength shift for growing biofilm in presence of different antibiotics. (g) SEM image of a Si_3N_4 grating supporting a GMR mode. (h) Resonance wavelength shift for an *E. coli* biofilm growing over the grating and later exposed to ciprofloxacin [128]. (i) Confocal microscopy showing an established biofilm (top panel) and confirming the disruption of the biofilm (bottom panel). Scale bar = 10 μm.

ability, in particular rifapentine [126]. Figure 7(f) plots the wavelength shift as a function of antibiotic, whereby a negative shift indicates sustained growth while a positive or zero shift indicates that biofilm is not fully forming. The partial efficacy of rifapentine is suggested by the negative shift in resonance wavelength of similar magnitude to that of an untreated sample (grey and red bars in Figure 7(f)). Biofilm formation is then inhibited more effectively by pairing rifapentine with a bactericidal drug, such as ampicillin or kanamycin, as evidenced by the black bar in Figure 7(f), which shows the smallest wavelength shift, indicative of no biofilm growth. Notably, the authors were

able to reach this conclusion in 2–3 h and with a relatively simple measurement configuration. This was enabled by the light confinement at the surface making the sensor sensitive only to the cell membrane of the first layer of bacteria, similar to other evanescent-wave sensors discussed in this section.

As an alternative to plasmonic resonances, we recently presented related work using GMRs excited in Si_3N_4 gratings (see Figure 7(g)). GMRs are quasi-guided modes excited in the near-wavelength regime of a grating [127]. Electromagnetic energy is confined in the slab, therefore resulting in the generation of an evanescent wave at the surface. The mode, however, can be readily coupled out to external radiation because of its leaky nature, which makes GMRs attractive because of the ease of measurement [20]. We exploited both the surface sensitivity and the spatial localization offered by the GMR mode to monitor the bottom layer of the biofilm as well as image the biofilm morphology and spatial distribution through hyperspectral imaging [128].

Similar to the plasmonic methods, the biofilm development and response to antibiotics was monitored at different time points, especially at the early stages of biofilm establishment. We showed that while some drugs may affect the top surface of the biofilm, they do not eradicate it. Conversely, antibiotics effective at destroying the biofilm, such as ciprofloxacin, caused a decrease of the resonance wavelength (see Figure 7(h)), thereby indicating that the bottom layer was being affected to the extent that it detached from the surface. The result was verified by confocal microscopy with live/dead staining, as shown in Figure 7(i), where alive bacteria appear green and dead ones appear red. Notably, the grating surface was not functionalized with any capture molecules and did not require any fluorescent labelling. These aspects are particularly important for real applications where the species of the biofilm-forming bacteria may not be known. In that case, functionalizing the surface with antibodies that target specific bacterial membrane proteins may miss the bacteria of interest. As a downside, the lack of functionalization delayed the attachment of the bacteria and their colonization of the surface.

These examples show that monitoring the first and arguably most important layer of the biofilm leads to the early detection of its formation. Furthermore, it allows monitoring very clearly the attack by some antimicrobials compared with traditional techniques that are destructive and require either lengthy and resource-consuming staining procedures or a confocal microscope to observe the bottom layer [129].

Overall, these techniques offer several interesting insights. First, physical changes induced by antibiotics to the bacterial membrane can be detected on a timescale shorter or comparable with that of growth by cell division, with the surface sensitivity being a particular asset. Second, sensing

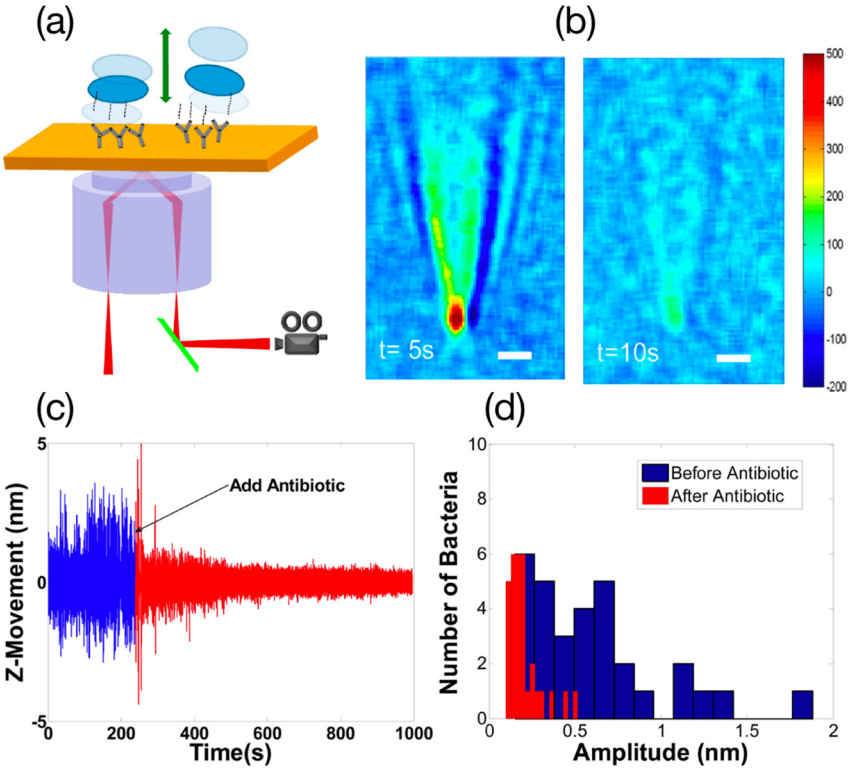

Figure 8: (a) Diagram of the SPR sensor demonstrate by Syal et al. [51]. (b) SPR contrast images of a single *Escherichia coli* tethered on the gold surface at different time points. Scale bars: 2 μm (c) *z*-movement of a single bacterium over time, before and after the addition of 0.5 mg/mL of polymyxin B. (d) Distribution of nanomotion amplitudes of different individual bacteria before (blue bars) and after (red bard) exposure to the antibiotic.

with a guided mode reduces time even for a growth assay because the guided mode is sensitive to a single layer of bacteria, therefore enabling the detection of bacterial division at a much lower bacterial concentration. Notably, none of the traditional microbiological techniques enables such an insightful observation and reduction in time.

Because of the increased sensitivity and reduction of detection time offered by sensing fewer bacteria with an evanescent tail, one would expect that pushing light-matter interaction to the level of individual bacteria would further reduce detection time. In fact, this reduction has been demonstrated by using SPRi [51]. As introduced in Section 2.1.4. The SPRi configuration, sketched in Figure 8(a), was used to monitor a single bacterium tethered to the surface via antibody binding. The contrast of the image fluctuates over time because of the motion of the bound bacteria as the bacterium moves within the evanescent tail of the resonant mode, as shown in Figure 8(b). The fluctuations in intensity can be converted into a z-movement of the bacterium because the exponential decay is well known (equation 1) and can be used to quantify the bacterial motion perpendicular to the surface.

After the exposure of tethered bacteria to 0.5 mg/mL of the antibiotic polymyxin B, the bacterial motion is almost immediately reduced to levels comparable with the fluctuations of dead bacteria, as illustrated in Figure 8(c). Although the authors ascribe the sudden decrease to the loss of viability and halting of the bacterial metabolism, it is important to note that the impressively rapid response is due to the very high concentration of antibiotic used, which corresponds to 25 times the MIC for polymyxin B. Nevertheless, when the bacteria are exposed to a near-MIC concentration, a similar response occurs within 1 h, which is still much faster than conventional tests. Moreover, the single-cell capability afforded by the SPRi method allows probing bacterial heterogeneity by studying the distribution of nanomotion amplitudes of tens of individual bacteria as shown in Figure 8(d).

The response time was also confirmed in later work from the same group, where the nanomotion was measured with a simple brightfield microscope. It was observed that a near-MIC of the same antibiotic, the decrease in nanomotion happened over 1–1.5 h [130]. Although this second configuration is inherently easier to operate, it can only detect 2D nanomotion across the plane where bacteria attach. Nevertheless, in this second work, the single-cell capability allowed the authors to distinguish subpopulations showing different sensitivities to the antibiotic administration. This is a clear example of heteroresistance, a phenomenon that, despite being crucial to characterizing the response of a bacterial population to an antibiotic treatment [11, 12, 131], is commonly neglected in traditional bulk experiments.

4 Conclusions

We have reviewed and critically assessed progress in the use of photonic and nanophotonic techniques for the detection and monitoring of bacteria. By comparing the more advanced sensing and imaging techniques against conventional methods, we have attempted to answer the question of what added value nanophotonics can bring to the detection of bacteria and, more specifically, to the global problem of antimicrobial resistance. How do nanophotonic techniques allow us to better assess the response of bacteria to antibiotic challenge, that is to assess their susceptibility?

Conventional techniques, such as the Kirby-Bauer test, used in every hospital laboratory are based on measuring the growth of entire bacterial colonies. Naturally, it takes at least an overnight incubation for bacteria to grow to a concentration that is detectable by visual inspection or quantifiable by a traditional OD measurement (OD_{600}) [96, 97, 132]. We refer to this is a "macroscopic" test. By observing the growth of fewer bacteria, we enter the "microscopic" regime, whereby changes in individual bacteria can be detected. A number of techniques, such as flow cytometry [114, 116], forward laser light scattering [26, 109] and nanostructure-enhanced methods [118, 121] can provide such microscopic information and allow us to reduce the assessment of susceptibility from 24–48 h down to 2–6 h (see Table 3), simply because they are able to observe a small number of bacteria rather than large colonies.

Reducing the spatial dimension further, we enter the "nanoscopic" domain, where only a part of the bacterium is interrogated, most notably the cell wall. Guided mode and resonant techniques such as those based on surface plasmons or dielectric resonances allow us to enter this regime because they are all based on the interaction between the evanescent tail of a confined mode and the outside of the bacterium. This reduction in scale gives a further reduction in assessment time, down to 0.5–2 h, as highlighted in Table 3. This further decrease is enabled by increasing the sensitivity to bacterial growth because only the first layer of adherent bacteria is probed by the evanescent tail [23, 122], therefore affording to probe growth from a much earlier stage. Such configuration lends itself to the study of real-time biofilm growth [125, 128], where the bottom layer is crucial, and represents an attractive alternative to traditional cumbersome microscopy or staining protocols [129].

In terms of sensitivity, we have also highlighted a number of techniques that successfully use interferometry to amplify the observation of bacterial presence. As is well known, phase-based measurements are among the most sensitive in photonics, so it is no surprise that this strategy is also successful in the detection and monitoring of a small number of bacteria, both for measuring low concentrations [68–70] and for assessing bacterial susceptibility to antibiotics [121].

Another parameter that is not picked up by culturing methods is the heterogeneity of the bacterial response. Bacteria, like any other living organism, exhibit heterogeneity, so it is an oversimplification to assume that they all respond in the same way. Ignoring heterogeneity is a mistake made by every averaging method such as culturing. In particular, it ignores the issue of heteroresistance and the presence of persister cells [10, 12]. Flow cytometry [114, 116] and droplet microfluidics [131] are already able to pick up heterogeneity, but only at the microscopic scale. We therefore see exciting opportunities for techniques such as SPRi [51] or GMR imaging [32, 79] to add their nanoscale sensing ability to this problem.

In addition, the strong light-bacterium interaction provided by nanoscopic techniques allows probing bacterial properties alternative to growth, with extreme sensitivity, that escape the traditional Kirby-Bauer test. A first example is the OD of the bacterial cell wall [22, 23], which was shown to be affected by antibiotics on a timescale comparable to or shorter than the bacterial division time. This suggests that changes to the cell wall become evident before the bacterium exhibits changes on a microscopic scale and represent a further avenue worth exploring for future ASTs. The OD of the cell wall was also exploited to identify different bacteria and classify Gram-positive and Gram-negative strains [21, 22].

Similar to the cell wall, the ability of bacteria to swim and colonize surfaces has been used as a signature of their viability, whereby a significant reduction in physical motion can be interpreted as an indicator of a successful antibiotic challenge. A number of articles we highlight [51, 118, 130] have demonstrated this phenomenon by using nanophotonic techniques and have also verified it against conventional susceptibility tests that nanomotion and motility are relatively fast (~1 h) indicators of susceptibility.

Altogether, these findings indicate that the ability to optically assess bacteria on a nanoscopic length scale allows us to observe antibiotic susceptibility on a biological timescale rather than on a timescale dictated by physical observation. This marks a profound change and improvement on the Kirby-Bauer test.

Importantly, we note that the advantage of using some of these indicators alternative to growth is also supported by other findings which do not necessarily use photonics, such as microfluidic techniques [25, 119, 133, 134], AFM cantilever deflection [24, 120, 135] or electrochemical platforms [136–138]. For example, bacterial metabolism drives ion-exchange across the membrane, so we see the measurement of electrical impedance at the single-cell level as a very promising method that could be added to the toolkit [90, 136]. These observations suggest that a synergistic approach between different domains is desirable, as it might be able to provide even greater insight and meet important needs that still pose challenges. For instance, microfluidics is crucial for tasks such as sample handling, filtration, delivery and enrichment while requiring low volumes of solutions [15, 28]. Therefore, further developments in microfluidics are expected to bring significant benefit to photonic biosensors. Bacterial identification is also challenging and currently requires lengthy cultivation and specialized personnel. In this respect, Raman [139–142] and IR spectroscopy [143, 144] represent promising alternative candidates to address the issue, while also being able to carry out susceptibility tests.

For these reasons, overall, we believe that the ideal bacterial detection and testing device will likely be multiparametric, thereby making it able to measure several parameters at the same time. In fact, it seems naive to assume that the diversity of the bacterial world can be captured by measuring a single parameter; similarly, antibiotics have many different modes of action. Antibiotic susceptibility is a multidimensional problem that can only be solved with a multiparameter approach. Several techniques have already recognized this need by measuring multiple responses in parallel, for example, morphology in conjunction with motility [25] or single-cell division [132, 133], electrical impedance with motility [90] or bacterial division [138], as well as growth and motility [118].

Photonics can play a significant role in this development roadmap, thanks to the desirable features we highlighted in this article. However, despite some of the conceptual leaps described here, no real major technological breakthrough has happened at the *clinical* level since Kirby and Bauer developed their disk diffusion test. This is due to some major hurdles that still need to be overcome to make these platforms suitable for translation into the clinic.

First, it is important to note that most of the photonic techniques discussed here only address part of the issues of current ASTs in terms of total assay time. In fact, an important bottleneck of current ASTs is the time needed for a clinical sample to be precultured to isolate a pure bacterial colony. All the photonic techniques presented here were

tested directly with a pure colony or a standardizes inoculum, namely a known bacterial strain which was cultured overnight and then suspended in a known medium [4, 5]. This implies that the reduction in assay time discussed throughout this review only concerns the time needed for the actual detection of susceptibility (termed drug test time in Table 3), not for the entire AST process. To reduce the entire assay time, a synergistic approach with microfluidics and other photonics identification techniques is expected to bring significant advantages, as discussed previously.

Second, such emerging devices ought to be made scalable and cost-effective. Reducing the optical probed volume often comes with the need of using nanostructures, whose fabrication requires electron beam lithography and cleanroom procedures, which are neither easy nor cost-effective to scale. Although significant progress has been made in this direction and many point of care detection platforms have been demonstrated [65, 145, 146], these devices still need to be validated for reproducible and accurate on-field operation. In addition, many portable technologies still suffer from insufficient sensitivity to be able to perform early diagnosis [147]. To this purpose, we expect technologies such as nanoimprint lithography, 3D printing and paper microfluidics to play important roles in nanostructures fabrication, sensor assembly and microfluidic circuitry realization, respectively. This will contribute to decreasing cost and making nanophotonic technologies easier to translate [148].

Finally, because many of these novel techniques are still emerging, they need to be extensively tested, both at the research level and in the clinic to meet the stringent requirements of regulatory bodies. These regulations entail lengthy and costly validations, which are however necessary to ensure safety, performance and low rates of errors. Broader targets of this testing include reproducibility, fidelity and applicability to the largest possible number of bacteria-drug combinations. In this context, closer collaborations with clinicians, microbiologists and health economists is of paramount importance to assess the viability of developed platforms and their impact on the health care system.

Author contribution: All the authors have accepted responsibility for the entire content of this submitted manuscript and approved submission.

Research funding: The authors acknowledge funding from the EPSRC (Grants EP/P030017/1 'Resonant and shaped photonics for understanding the physical and biomedical world' and EP/P02324X/1 'Multiparameter Assay for Profiling Susceptibility (MAPS)'). Prof. Thomas F. Krauss acknowledges the Royal Society Wolfson Research Merit Award Scheme.

Conflict of interest statement: The authors declare no conflicts of interest regarding this article.

References

[1] S. M. Yoo and S. Y. Lee, "Optical biosensors for the detection of pathogenic microorganisms," *Trends Biotechnol.*, vol. 34, pp. 7–25, 2016.

[2] A. Ahmed, J. V. Rushworth, N. A. Hirst, and P. A. Millner, "Biosensors for whole-cell bacterial detection," *Clin. Microbiol. Rev.*, vol. 27, pp. 631–646, 2014.

[3] J. de Dieu Habimana, J. Ji, and X. Sun, "Minireview: trends in optical-based biosensors for point-of-care bacterial pathogen detection for food safety and clinical diagnostics," *Anal. Lett.*, vol. 51, pp. 2933–2966, 2018.

[4] A. van Belkum, C. D. Burnham, J. W. A. Rossen, F. Mallard, O. Rochas, and W. M. Dunne, Jr., "Innovative and rapid antimicrobial susceptibility testing systems," *Nat. Rev. Microbiol.*, vol. 18, no. 5, pp. 299–311, 2020.

[5] A. van Belkum, T. T. Bachmann, G. Lüdke, et al., "Developmental roadmap for antimicrobial susceptibility testing systems," *Nat. Rev. Microbiol.*, vol. 17, pp. 51–62, 2019.

[6] J. O'Neill, "Review on antimicrobial resistance. Tackling a global health crisis: rapid diagnostics: stopping unnecessary use of antibiotics," *Indep. Rev. AMR*, pp. 1–36, 2015.

[7] X. Wang, Y. Kang, L. Luo, et al., "Heteroresistance at the single-cell level: adapting to antibiotic stress through a population-based strategy and growth-controlled," *mBio*, vol. 5, pp. 1–9, 2014.

[8] V. I. Band, E. K. Crispell, B. A. Napier, et al., "Antibiotic failure mediated by a resistant subpopulation in *Enterobacter cloacae*," *Nat. Microbiol.*, vol. 1, 2016, https://doi.org/10.1038/nmicrobiol.2016.53.

[9] F. Lyu, M. Pan, S. Patil, et al., "Phenotyping antibiotic resistance with single-cell resolution for the detection of heteroresistance," *Sensors Actuators B Chem.*, vol. 270, pp. 396–404, 2018.

[10] N. Q. Balaban, J. Merrin, R. Chait, L. Kowalik, and S. Leibler, "Bacterial persistence as a phenotypic switch," *Science*, vol. 305, pp. 1622–1625, 2004.

[11] H. Nicoloff, K. Hjort, B. R. Levin, and D. I. Andersson, "The high prevalence of antibiotic heteroresistance in pathogenic bacteria is mainly caused by gene amplification," *Nat. Microbiol.*, vol. 4, pp. 504–514, 2019.

[12] D. I. Andersson, H. Nicoloff, and K. Hjort, "Mechanisms and clinical relevance of bacterial heteroresistance," *Nat. Rev. Microbiol.*, vol. 17, pp. 479–496, 2019.

[13] M. E. Lidstrom and M. C. Konopka, "The role of physiological heterogeneity in microbial population behavior," *Nat. Chem. Biol.*, vol. 6, pp. 705–712, 2010.

[14] K. M. Davis and R. R. Isberg, "Defining heterogeneity within bacterial populations via single cell approaches," *Bioessays*, vol. 38, pp. 782–790, 2016.

[15] H. Yin and D. Marshall, "Microfluidics for single cell analysis," *Curr. Opin. Biotechnol.*, vol. 23, pp. 110–119, 2012.

[16] P. Mehrotra, B. Chatterjee, and S. Sen, "EM-wave biosensors: a review of RF, microwave, mm-wave and optical sensing," *Sensors*, vol. 19, 2019, https://doi.org/10.3390/s19051013.

[17] E. A. Specht, E. Braselmann, and A. E. Palmer, "A critical and comparative review of fluorescent tools for live-cell imaging," *Annu. Rev. Physiol.*, vol. 79, pp. 93–117, 2017.
[18] D. G. Allison and M. A. Sattenstall, "The influence of green fluorescent protein incorporation on bacterial physiology: a note of caution," *J. Appl. Microbiol.*, vol. 103, pp. 318–324, 2007.
[19] S. Rapposch, P. Zangerl, and W. Ginzinger, "Influence of fluorescence of bacteria stained with acridine orange on the enumeration of microorganisms in raw milk," *J. Dairy Sci.*, vol. 83, pp. 2753–2758, 2000.
[20] G. Pitruzzello and T. F. Krauss, "Photonic crystal resonances for sensing and imaging," *J. Opt.*, vol. 20, p. 073004, 2018.
[21] M. Tardif, J.-B. Jager, P. R. Marcoux, et al., "Single-cell bacterium identification with a SOI optical microcavity," *Appl. Phys. Lett.*, vol. 109, 2016, https://doi.org/10.1063/1.4963070.
[22] R. Therisod, M. Tardif, P. R. Marcoux, et al., "Gram-type differentiation of bacteria with 2D hollow photonic crystal cavities," *Appl. Phys. Lett.*, vol. 113, 2018, https://doi.org/10.1063/1.5037849.
[23] Y. L. Chiang, C. H. Lin, M. Y. Yen, Y. D. Su, S. J. Chen, and H. Chen, "Innovative antimicrobial susceptibility testing method using surface plasmon resonance," *Biosens. Bioelectron.*, vol. 24, pp. 1905–1910, 2009.
[24] G. Longo, L. Alonso-Sarduy, L. M. Rio, et al., "Rapid detection of bacterial resistance to antibiotics using AFM cantilevers as nanomechanical sensors," *Nat. Nanotechnol.*, vol. 8, pp. 522–526, 2013.
[25] G. Pitruzzello, S. Thorpe, S. Johnson, A. Evans, H. Gadêlha, and T. F. Krauss, "Multiparameter antibiotic resistance detection based on hydrodynamic trapping of individual *E. coli*," *Lab Chip*, vol. 19, pp. 1417–1426, 2019.
[26] R. T. Hayden, L. K. Clinton, C. Hewitt, et al., "Rapid antimicrobial susceptibility testing using forward laser light scatter technology," *J. Clin. Microbiol.*, vol. 54, pp. 2701–2706, 2016.
[27] Z. Mohammed, E. Sauna, and A. Turner, *Principles of Bacterial Detection: Biosensors, Recognition Receptors and Microsystem*, Berlin, Germany, Springer Science & Business Media, 2008.
[28] G. M. Whitesides, "The origins and the future of microfluidics," *Nature*, vol. 442, pp. 368–373, 2006.
[29] D. R. Reyes, D. Iossifidis, P.-A. Auroux, and A. Manz, "Micro total analysis systems. 1. Introduction, theory, and technology," *Anal. Chem.*, vol. 74, pp. 2623–2636, 2002.
[30] P.-A. Auroux, D. Iossifidis, D. R. Reyes, and A. Manz, "Micro total analysis systems. 2. Analytical standard operations and applications," *Anal. Chem.*, vol. 74, pp. 2637–2652, 2002.
[31] P. Dey, N. Fabri-Faja, O. Calvo-Lozano, et al., "Label-free bacteria quantification in blood plasma by a bioprinted microarray based interferometric point-of-care device," *ACS Sensors*, vol. 4, pp. 52–60, 2019.
[32] D. Conteduca I. Barth, G. Pitruzzello, C. Reardon, E. Martins, T. Krauss, "Dielectric nanohole array metasurface for high-resolution near-field sensing and imaging," *Under Review*, 2020, https:/doi.org/10.21203/rs.3.rs-44521/v1.
[33] A. van Leewenhoeck, "Observations, communicated to the publisher by Mr. Antony van Leewenhoeck, in a Dutch letter of the 9th Octob. 1676. here English'd: concerning little animals by him observed in rain-well-sea- and snow water; as also in water wherein pepper had lain infus," *Philos. Trans. R. Soc. London*, vol. 12, pp. 821–831, 1677.
[34] Z. Yu and S. Fan, "Extraordinarily high spectral sensitivity in refractive index sensors using multiple optical modes," *Opt. Express*, vol. 19, p. 10029, 2011.
[35] J. Homola, "Surface plasmon resonance sensors for detection of chemical and biological species," *Chem. Rev.*, vol. 108, pp. 462–493, 2008.
[36] N. Tawil, E. Sacher, R. Mandeville, and M. Meunier, "Surface plasmon resonance detection of *E. coli* and methicillin-resistant *S. aureus* using bacteriophages," *Biosens. Bioelectron.*, vol. 37, pp. 24–29, 2012.
[37] E. Özgür, A. A. Topçu, E. Yılmaz, and A. Denizli, "Surface plasmon resonance based biomimetic sensor for urinary tract infections," *Talanta*, vol. 212, p. 120778, 2020.
[38] S. Nair, J. Gomez-Cruz, Á. Manjarrez-Hernandez, G. Ascanio, R. G. Sabat, and C. Escobedo, "Selective uropathogenic *E. coli* detection using crossed surface-relief gratings," *Sensors*, vol. 18, pp. 1–12, 2018.
[39] C. Escobedo, "On-chip nanohole array based sensing: a review," *Lab Chip*, vol. 13, pp. 2445–2463, 2013.
[40] X. Li, M. Soler, C. I. Özdemir, A. Belushkin, F. Yesilköy, and H. Altug, "Plasmonic nanohole array biosensor for label-free and real-time analysis of live cell secretion," *Lab Chip*, vol. 17, pp. 2208–2217, 2017.
[41] M. Soler, A. Belushkin, A. Cavallini, C. Kebbi-Beghdadi, G. Greub, and H. Altug, "Multiplexed nanoplasmonic biosensor for one-step simultaneous detection of *Chlamydia trachomatis* and *Neisseria gonorrhoeae* in urine," *Biosens. Bioelectron.*, vol. 94, pp. 560–567, 2017.
[42] J. Gomez-Cruz, S. Nair, A. Manjarrez-Hernandez, S. Gavilanes-Parra, G. Ascanio, and C. Escobedo, "Cost-effective flow-through nanohole array-based biosensing platform for the label-free detection of uropathogenic *E. coli* in real time," *Biosens. Bioelectron.*, vol. 106, pp. 105–110, 2018.
[43] I. Barth, D. Conteduca, C. Reardon, S. Johnson, and T. F. Krauss, "Common-path interferometric label-free protein sensing with resonant dielectric nanostructures," *Light Sci. Appl.*, vol. 9, p. 96, 2020.
[44] G. Steiner, "Surface plasmon resonance imaging," *Anal. Bioanal. Chem.*, vol. 379, pp. 328–331, 2004.
[45] S. Bouguelia, Y. Roupioz, S. Slimani, et al., "On-chip microbial culture for the specific detection of very low levels of bacteria," *Lab Chip*, vol. 13, p. 4024, 2013.
[46] M. Boulade, A. Morlay, F. Piat, et al., "Early detection of bacteria using SPR imaging and event counting: experiments with *Listeria monocytogenes* and *Listeria innocua*," *RSC Adv.*, vol. 9, pp. 15554–15560, 2019.
[47] L. Laplatine, L. Leroy, R. Calemczuk, et al., "Spatial resolution in prism-based surface plasmon resonance microscopy," *Opt. Express*, vol. 22, p. 22771, 2014.
[48] C. E. H. Berger, R. P. H. Kooyman, and J. Greve, "Resolution in surface plasmon microscopy," *Rev. Sci. Instrum.*, vol. 65, pp. 2829–2836, 1994.
[49] G. Stabler, M. G. Somekh, and C. W. See, "High-resolution wide-field surface plasmon microscopy," *J. Microsc.*, vol. 214, pp. 328–333, 2004.
[50] B. Huang, F. Yu, and R. N. Zare, "Surface plasmon resonance imaging using a high numerical aperture microscope objective," *Anal. Chem.*, vol. 79, pp. 2979–2983, 2007.

[51] K. Syal, R. Iriya, Y. Yang, et al., "Antimicrobial susceptibility test with plasmonic imaging and tracking of single bacterial motions on nanometer scale," *ACS Nano*, vol. 10, pp. 845–852, 2016.
[52] S. Wang, X. Shan, U. Patel, et al., "Label-free imaging, detection, and mass measurement of single viruses by surface plasmon resonance," *Proc. Natl. Acad. Sci. U. S. A.*, vol. 107, pp. 16028–16032, 2010.
[53] W. Wang, Y. Yang, S. Wang, et al., "Label-free measuring and mapping of binding kinetics of membrane proteins in single living cells," *Nat. Chem.*, vol. 4, pp. 846–853, 2012.
[54] Y. Yang, H. Yu, X. Shan, et al., "Label-free tracking of single organelle transportation in cells with nanometer precision using a plasmonic imaging technique," *Small*, vol. 11, pp. 2878–2884, 2015.
[55] S. Nair, J. Gomez-Cruz, Á. Manjarrez-Hernandez, G. Ascanio, R. G. Sabat, and C. Escobedo, "Rapid label-free detection of intact pathogenic bacteria: in situ via surface plasmon resonance imaging enabled by crossed surface relief gratings," *Analyst*, vol. 145, pp. 2133–2142, 2020.
[56] A. Ashkin, J. M. Dziedzic, and T. Yamane, "Optical trapping and manipulation of single cells using," *Nature*, vol. 330, pp. 769–711, 1987.
[57] A. Ashkin and J. M. Dziedzic, "Optical trapping and manipulation of viruses and bacteria," *Science*, vol. 235, pp. 1517–1520, 1987.
[58] D. Conteduca, F. Dell'Olio, T. F. Krauss, and C. Ciminelli, "Photonic and plasmonic nanotweezing of nano- and microscale particles," *Appl. Spectrosc.*, vol. 71, pp. 367–390, 2017.
[59] O. Lotan, J. Bar-David, C. L. C. Smith, et al., "Nanoscale plasmonic V-groove waveguides for the interrogation of single fluorescent bacterial cells," *Nano Lett.*, vol. 17, pp. 5481–5488, 2017.
[60] Y. Pang and R. Gordon, "Optical trapping of a single protein," *Nano Lett.*, vol. 12, pp. 402–406, 2012.
[61] M. Righini, P. Ghenuche, S. Cherukulappurath, V. Myroshnychenko, F. J. García de Abajo, and R. Quidant, "Nano-optical trapping of Rayleigh particles and *Escherichia coli* bacteria with resonant optical antennas," *Nano Lett.*, vol. 9, pp. 3387–3391, 2009.
[62] K. C. Neuman, E. H. Chadd, G. F. Liou, K. Bergman, and S. M. Block, "Characterization of photodamage to *Escherichia coli* in optical traps," *Biophys. J.*, vol. 77, pp. 2856–2863, 1999.
[63] M. B. Rasmussen, L. B. Oddershede, and H. Siegumfeldt, "Optical tweezers cause physiological damage to *Escherichia coli* and *Listeria bacteria*," *Appl. Environ. Microbiol.*, vol. 74, pp. 2441–2446, 2008.
[64] D. Threm, Y. Nazirizadeh, and M. Gerken, "Photonic crystal biosensors towards on-chip integration," *J. Biophotonics*, vol. 5, pp. 601–616, 2012.
[65] H. Inan, M. Poyraz, F. Inci, et al., "Photonic crystals: emerging biosensors and their promise for point-of-care applications," *Chem. Soc. Rev.*, vol. 46, pp. 366–388, 2017.
[66] R. Horváth, H. C. Pedersen, N. Skivesen, D. Selmeczi, and N. B. Larsen, "Optical waveguide sensor for on-line monitoring of bacteria," *Opt. Lett.*, vol. 28, p. 1233, 2003.
[67] D. Sarkar, N. S. K. Gunda, I. Jamal, and S. K. Mitra, "Optical biosensors with an integrated Mach-Zehnder Interferometer for detection of *Listeria monocytogenes*," *Biomed. Microdevices*, vol. 16, pp. 509–520, 2014.
[68] J. Maldonado, A. B. González-Guerrero, C. Domínguez, and L. M. Lechuga, "Label-free bimodal waveguide immunosensor for rapid diagnosis of bacterial infections in cirrhotic patients," *Biosens. Bioelectron.*, vol. 85, pp. 310–316, 2016.
[69] J. Maldonado, M.-C. Estévez, A. Fernández-Gavela, J. J. González-López, A. B. González-Guerrero, and L. M. Lechuga, "Label-free detection of nosocomial bacteria using a nanophotonic interferometric biosensor," *Analyst*, vol. 145, pp. 497–506, 2020.
[70] S. Kaushik, U. Tiwari, Nilima, S. Prashar, B. Das, and R. K. Sinha, "Label-free detection of *Escherichia coli* bacteria by cascaded chirped long period gratings immunosensor," *Rev. Sci. Instrum.*, vol. 90, 2019.
[71] M. Janik, M. Koba, A. Celebańska, W. J. Bock, and M. Śmietana, "Live *E. coli* bacteria label-free sensing using a microcavity in-line Mach-Zehnder interferometer," *Sci. Rep.*, vol. 8, pp. 4–11, 2018.
[72] S. Kaushik, U. K. Tiwari, S. S. Pal, and R. K. Sinha, "Rapid detection of *Escherichia coli* using fiber optic surface plasmon resonance immunosensor based on biofunctionalized Molybdenum disulfide (MoS 2) nanosheets," *Biosens. Bioelectron.*, vol. 126, pp. 501–509, 2019.
[73] C. Ribaut, M. Loyez, J. C. Larrieu, et al., "Cancer biomarker sensing using packaged plasmonic optical fiber gratings: towards in vivo diagnosis," *Biosens. Bioelectron.*, vol. 92, pp. 449–456, 2017.
[74] S.-H. Ohk and A. K. Bhunia, "Multiplex fiber optic biosensor for detection of *Listeria monocytogenes*, *Escherichia coli* O157:H7 and *Salmonella enterica* from ready-to-eat meat samples," *Food Microbiol.*, vol. 33, pp. 166–171, 2013.
[75] N. Li, X. R. Cheng, A. Brahmendra, et al., "Photonic crystals on copolymer film for bacteria detection," *Biosens. Bioelectron.*, vol. 41, pp. 354–358, 2013.
[76] G. Murtaza, A. S. Rizvi, M. Irfan, et al., "Glycated albumin based photonic crystal sensors for detection of lipopolysaccharides and discrimination of Gram-negative bacteria," *Anal. Chim. Acta*, vol. 1117, pp. 1–8, 2020.
[77] Z. Cai, D. H. Kwak, D. Punihaole, et al., "A photonic crystal protein hydrogel sensor for *Candida albicans*," *Angew. Chem.*, vol. 54, pp. 13036–13040, 2015.
[78] L. Tilton, G. Das, X. Yang, N. Wisuthiphaet, I. M. Kennedy, and N. Nitin, "Nanophotonic device in combination with bacteriophages for enhancing detection sensitivity of *Escherichia coli* in simulated wash water," *Anal. Lett.*, vol. 52, pp. 2203–2213, 2019.
[79] J. Juan-Colás, I. S. Hitchcock, M. Coles, S. Johnson, and T. F. Krauss, "Quantifying single-cell secretion in real time using resonant hyperspectral imaging," *Proc. Natl. Acad. Sci. U. S. A.*, vol. 115, pp. 13204–13209, 2018.
[80] Y. Zhuo, J. S. Choi, T. Marin, H. Yu, B. A. Harley, and B. T. Cunningham, "Quantitative analysis of focal adhesion dynamics using photonic resonator outcoupler microscopy (PROM)," *Light Sci. Appl.*, vol. 7, pp. 1–15, 2018.
[81] Z. Xu, W. Song, and K. B. Crozier, "Optical trapping of nanoparticles using all-silicon nanoantennas," *ACS Photonics*, vol. 5, pp. 4993–5001, 2018.
[82] D. Erickson, X. Serey, Y. F. Chen, and S. Mandal, "Nanomanipulation using near field photonics," *Lab Chip*, vol. 11, pp. 995–1009, 2011.
[83] A. H. J. Yang, S. D. Moore, B. S. Schmidt, M. Klug, M. Lipson, and D. Erickson, "Optical manipulation of nanoparticles and biomolecules in sub-wavelength slot waveguides," *Nature*, vol. 457, pp. 71–75, 2009.

[84] C. Pin, J. B. Jager, M. Tardif, et al., "Optical tweezing using tunable optical lattices along a few-mode silicon waveguide," *Lab Chip*, vol. 18, pp. 1750–1757, 2018.
[85] H. Zhao, L. K. Chin, Y. Shi, et al., "Massive nanophotonic trapping and alignment of rod-shaped bacteria for parallel single-cell studies," *Sensors Actuators B Chem.*, vol. 306, p. 127562, 2020.
[86] N. Descharmes, U. P. Dharanipathy, Z. Diao, M. Tonin, and R. Houdré, "Observation of backaction and self-induced trapping in a planar hollow photonic crystal cavity," *Phys. Rev. Lett.*, vol. 110, p. 123601, 2013.
[87] T. Van Leest and J. Caro, "Cavity-enhanced optical trapping of bacteria using a silicon photonic crystal," *Lab Chip*, vol. 13, pp. 4358–4365, 2013.
[88] J. Juan-Colás, A. Parkin, K. E. Dunn, M. G. Scullion, T. F. Krauss, and S. D. Johnson, "The electrophotonic silicon biosensor," *Nat. Commun.*, vol. 7, pp. 1–7, 2016.
[89] J. Juan-Colás, T. F. Krauss, and S. D. Johnson, "Real-time analysis of molecular conformation using silicon electrophotonic biosensors," *ACS Photonics*, vol. 4, pp. 2320–2326, 2017.
[90] D. Conteduca, G. Brunetti, F. Dell'Olio, M. N. Armenise, T. F. Krauss, and C. Ciminelli, "Monitoring of individual bacteria using electro-photonic traps," *Biomed. Opt. Express*, vol. 10, p. 3463, 2019.
[91] H. Xin, Q. Liu, and B. Li, "Non-contact fiber-optical trapping of motile bacteria: dynamics observation and energy estimation," *Sci. Rep.*, vol. 3, pp. 1–8, 2014.
[92] M. Tardif, J. B. Jager, P. R. Marcoux, et al., "Single-cell bacterium identification with a SOI optical microcavity," *Appl. Phys. Lett.*, vol. 109, 2016.
[93] J. C. Lagier, S. Edouard, I. Pagnier, O. Mediannikov, M. Drancourt, and D. Raoult, "Current and past strategies for bacterial culture in clinical microbiology," *Clin. Microbiol. Rev.*, vol. 28, pp. 208–236, 2015.
[94] J. H. Jorgensen and M. J. Ferraro, "Antimicrobial susceptibility testing: a review of general principles and contemporary practices," *Clin. Infect. Dis.*, vol. 49, pp. 1749–1755, 2009.
[95] B. Behera, G. K. Anil Vishnu, S. Chatterjee, et al., "Emerging technologies for antibiotic susceptibility testing," *Biosens. Bioelectron.*, vol. 142, 2019.
[96] A. W. Bauer, "Single-disk antibiotic-sensitivity testing of staphylococci," *AMA Arch. Intern. Med.*, vol. 104, p. 208, 1959.
[97] C. A. Rotilie, R. J. Fass, R. B. Prior, and R. L. Perkins, "Microdilution technique for antimicrobial susceptibility testing of anaerobic bacteria," *Antimicrob. Agents Chemother.*, vol. 7, pp. 311–315, 2012.
[98] D. H. Pincus, "Microbial identification using the bioMérieux VITEK® 2 system," *Encycl. Rapid Microbiol. Methods*, pp. 1–32, 2010.
[99] A. McGregor, F. Schio, S. Beaton, V. Boulton, M. Perman, and G. Gilbert, "The microscan walkaway diagnostic microbiology system — An evaluation," *Pathology*, vol. 27, pp. 172–176, 1995.
[100] K. C. Carroll, B. D. Glanz, A. P. Borek, et al., "Evaluation of the BD Phoenix automated microbiology system for identification and antimicrobial susceptibility testing of *Enterobacteriaceae*," *J. Clin. Microbiol.*, vol. 44, pp. 3506–3509, 2006.
[101] A. Lupetti, S. Barnini, B. Castagna, P. H. Nibbering, and M. Campa, "Rapid identification and antimicrobial susceptibility testing of Gram-positive cocci in blood cultures by direct inoculation into the BD phoenix system," *Clin. Microbiol. Infect.*, vol. 16, pp. 986–991, 2010.
[102] M. Ligozzi, S. Barnini, B. Castagna, A. L. Capria, and P. H. Nibbering, "Rapid identification and antimicrobial susceptibility profiling of Gram-positive cocci in blood cultures with the Vitek 2 system," *Eur. J. Clin. Microbiol. Infect. Dis.*, vol. 40, pp. 89–95, 2002.
[103] F. Garcia-Garrote, E. Cercenado, and E. Bouza, "Evaluation of a new system, VITEK 2, for identification and antimicrobial susceptibility testing of enterococci," *J. Clin. Microbiol.*, vol. 38, pp. 2108–2111, 2000.
[104] J. L. Burns, L. Saiman, S. Whittier, et al., "Comparison of two commercial systems (Vitek and MicroScan-WalkAway) for antimicrobial susceptibility testing of *Pseudomonas aeruginosa* isolates from cystic fibrosis patients," *Diagn. Microbiol. Infect. Dis.*, vol. 39, pp. 257–260, 2001.
[105] H. S. Sader, T. R. Fritsche, and R. N. Jones, "Accuracy of three automated systems (MicroScan WalkAway, VITEK, and VITEK 2) for susceptibility testing of," *Society*, vol. 44, pp. 1101–1104, 2006.
[106] C. Kulah, E. Aktas, F. Comert, N. Ozlu, I. Akyar, and H. Ankarali, "Detecting imipenem resistance in *Acinetobacter baumannii* by automated systems (BD Phoenix, Microscan WalkAway, Vitek 2); high error rates with Microscan WalkAway," *BMC Infect. Dis.*, vol. 9, pp. 1–7, 2009.
[107] E. A. Idelevich, D. A. Freeborn, H. Seifert, and K. Becker, "Comparison of tigecycline susceptibility testing methods for multidrug-resistant *Acinetobacter baumannii*," *Diagn. Microbiol. Infect. Dis.*, vol. 91, pp. 360–362, 2018.
[108] R. M. Berkman, P. J. Wyatt, and D. T. Phillips, "Rapid detection of penicillin sensitivity in *Staphylococcus aureus*," *Nature*, vol. 228, pp. 458–460, 1970.
[109] J. Murray, P. Evans, and D. W. L. Hukins, "Light-scattering methods for antibiotic sensitivity tests," *J. Clin. Pathol.*, vol. 33, pp. 995–1001, 1980.
[110] A. L. Roberts, U. Joneja, T. Villatoro, E. Andris, J. A. Boyle, and J. Bondi, "Evaluation of the BacterioScan 216Dx for standalone preculture screen of preserved urine specimens in a clinical setting," *Lab. Med.*, vol. 49, pp. 35–40, 2018.
[111] F. Hassan, H. Bushnell, C. Taggart, et al., "Evaluation of BacterioScan 216Dx in comparison to urinalysis as a screening tool for diagnosis of urinary tract infections in children," *J. Clin. Microbiol.*, vol. 57, pp. 1–7, 2019.
[112] J. V. Bugrysheva, C. Lascols, D. Sue, and L. M. Weigel, "Rapid antimicrobial susceptibility testing of *Bacillus anthracis*, *Yersinia pestis*, and *Burkholderia pseudomallei* by use of laser light scattering technology," *J. Clin. Microbiol.*, vol. 54, pp. 1462–1471, 2016.
[113] E. A. Idelevich, M. Hoy, D. Knaack, et al., "Direct determination of carbapenem-resistant *Enterobacteriaceae* and *Pseudomonas aeruginosa* from positive blood cultures using laser scattering technology," *Int. J. Antimicrob. Agents*, vol. 51, pp. 221–226, 2018.
[114] M. A. C. Broeren, Y. Maas, E. Retera, and N. L. A. Arents, "Antimicrobial susceptibility testing in 90 min by bacterial cell count monitoring," *Clin. Microbiol. Infect.*, vol. 19, pp. 286–291, 2013.
[115] T. H. Huang, Y. L. Tzeng, and R. M. Dickson, "FAST: rapid determinations of antibiotic susceptibility phenotypes using label-free cytometry," *Cytometry A*, vol. 93, pp. 639–648, 2018.

[116] D. Fonseca e Silva, A. Silva-Dias, R. Gomes, et al., "Evaluation of rapid colistin susceptibility directly from positive blood cultures using a flow cytometry assay," *Int. J. Antimicrob. Agents*, vol. 54, pp. 820–823, 2019.
[117] L. Yang, Y. Zhou, S. Zhu, T. Huang, L. Wu, and X. Yan, "Detection and quantification of bacterial autofluorescence at the single-cell level by a laboratory-built high-sensitivity flow cytometer," *Anal. Chem.*, vol. 84, pp. 1526–1532, 2012.
[118] D. Volbers, V. K. Stierle, K. J. Ditzel, et al., "Interference disturbance analysis enables single-cell level growth and mobility characterization for rapid antimicrobial susceptibility testing," *Nano Lett*, vol. 9, no. 2, pp. 643–651, 2019.
[119] V. Kara, C. Duan, K. Gupta, S. Kurosawa, D. J. Stearns-Kurosawa, and K. L. Ekinci, "Microfluidic detection of movements of *Escherichia coli* for rapid antibiotic susceptibility testing," *Lab Chip*, vol. 18, pp. 743–753, 2018.
[120] H. Etayash, M. F. Khan, K. Kaur, and T. Thundat, "Microfluidic cantilever detects bacteria and measures their susceptibility to antibiotics in small confined volumes," *Nat. Commun.*, vol. 7, p. 12947, 2016.
[121] H. Leonard, S. Halachmi, N. Ben-Dov, O. Nativ, and E. Segal, "Unraveling antimicrobial susceptibility of bacterial networks on micropillar architectures using intrinsic phase-shift spectroscopy," *ACS Nano*, vol. 11, pp. 6167–6177, 2017.
[122] J. S. Kee, S. Y. Lim, A. P. Perera, Y. Zhang, and M. K. Park, "Plasmonic nanohole arrays for monitoring growth of bacteria and antibiotic susceptibility test," *Sensors Actuators B Chem.*, vol. 182, pp. 576–583, 2013.
[123] S. Szunerits and R. Boukherroub, "Sensing using localised surface plasmon resonance sensors," *Chem. Commun.*, vol. 48, pp. 8999–9010, 2012.
[124] E. Petryayeva and U. J. Krull, "Localized surface plasmon resonance: nanostructures, bioassays and biosensing – A review," *Anal. Chim. Acta*, vol. 706, pp. 8–24, 2011.
[125] R. Funari, N. Bhalla, K. Y. Chu, B. Söderström, and A. Q. Shen, "Nanoplasmonics for real-time and label-free monitoring of microbial biofilm formation," *ACS Sensors*, vol. 3, pp. 1499–1509, 2018.
[126] M. C. Maher, J. Y. Lim, C. Gunawan, and L. Cegelski, "Cell-based high-throughput screening identifies rifapentine as an inhibitor of amyloid and biofilm formation in *Escherichia coli*," *ACS Infect. Dis.*, vol. 1, pp. 460–468, 2016.
[127] S. S. Wang and R. Magnusson, "Theory and applications of guided-mode resonance filters," *Appl. Opt.*, vol. 32, p. 2606, 1993.
[128] Y. Wang, C. P. Reardon, N. Read, et al. "Attachment and antibiotic response of early-stage biofilms studied using resonant hyperspectral imaging," *Under Review*, https://arxiv.org/abs/2009.03451.
[129] F. Pantanella, P. Valenti, T. Natalizi, D. Passeri, and F. Berlutti, "Analytical techniques to study microbial biofilm on abiotic surfaces: Pros and cons of the main techniques currently in use," *Ann. Ig.*, vol. 25, pp. 31–42, 2013.
[130] K. Syal, S. Shen, Y. Yang, S. Wang, S. E. Haydel, and N. Tao, "Rapid antibiotic susceptibility testing of uropathogenic *E. coli* by tracking submicron scale motion of single bacterial cells," *ACS Sensors*, vol. 2, pp. 1231–1239, 2017.
[131] O. Scheler, K. Makuch, P. R. Debski, et al., "Droplet-based digital antibiotic susceptibility screen reveals single-cell clonal heteroresistance in an isogenic bacterial population," *Sci. Rep.*, vol. 10, pp. 1–8, 2020.
[132] J. Choi, J. Yoo, M. Lee, et al., "A rapid antimicrobial susceptibility test based on single-cell morphological analysis," *Sci. Transl. Med.*, vol. 6, p. 267ra174, 2014.
[133] B. Li, Y. Qiu, A. Glidle, et al., "Gradient microfluidics enables rapid bacterial growth inhibition testing," *Anal. Chem.*, vol. 86, pp. 3131–3137, 2014.
[134] Ö. Baltekin, A. Boucharin, E. Tano, D. I. Andersson, and J. Elf, "Antibiotic susceptibility testing in less than 30 min using direct single-cell imaging," *Proc. Natl. Acad. Sci. U. S. A.*, vol. 114, pp. 9170–9175, 2017.
[135] S. Kasas, F. S. Ruggeri, C. Benadiba, et al., "Detecting nanoscale vibrations as signature of life," *Proc. Natl. Acad. Sci. U. S. A.*, vol. 112, pp. 378–381, 2015.
[136] M. Mallén-Alberdi, N. Vigués, J. Mas, C. Fernández-Sánchez, and A. Baldi, "Impedance spectral fingerprint of *E. coli* cells on interdigitated electrodes: a new approach for label free and selective detection," *Sens. Bio-Sensing Res.*, vol. 7, pp. 100–106, 2016.
[137] A. Rohani, J. H. Moore, Y. H. Su, V. Stagnaro, C. Warren, and N. S. Swami, "Single-cell electro-phenotyping for rapid assessment of *Clostridium difficile* heterogeneity under vancomycin treatment at sub-MIC (minimum inhibitory concentration) levels," *Sensors Actuators B Chem*, vol. 276, pp. 472–480, 2018.
[138] Y. Yang, K. Gupta, and K. L. Ekinci, "All-electrical monitoring of bacterial antibiotic susceptibility in a microfluidic device," *Proc. Natl. Acad. Sci. U. S. A.*, vol. 117, no. 20, pp. 10639–10644, 2020.
[139] D. Cialla-May, X. S. Zheng, K. Weber, and J. Popp, "Recent progress in surface-enhanced Raman spectroscopy for biological and biomedical applications: from cells to clinics," *Chem. Soc. Rev.*, vol. 46, pp. 3945–3961, 2017.
[140] B. Lorenz, C. Wichmann, S. Stöckel, P. Rösch, and J. Popp, "Cultivation-free Raman spectroscopic investigations of bacteria," *Trends Microbiol.*, vol. 25, pp. 413–424, 2017.
[141] A. Tannert, R. Grohs, J. Popp, and U. Neugebauer, "Phenotypic antibiotic susceptibility testing of pathogenic bacteria using photonic readout methods: recent achievements and impact," *Appl. Microbiol. Biotechnol.*, vol. 103, pp. 549–566, 2019.
[142] V. O. Baron, M. Chen, B. Hammarstrom, et al., "Real-time monitoring of live mycobacteria with a microfluidic acoustic-Raman platform," *Commun. Biol.*, vol. 3, pp. 1–8, 2020.
[143] W. Adamus-Białek, Ł. Lechowicz, A. B. Kubiak-Szeligowska, M. Wawszczak, E. Kamińska, and M. Chrapek, "A new look at the drug-resistance investigation of uropathogenic *E. coli* strains," *Mol. Biol. Rep.*, vol. 44, pp. 191–202, 2017.
[144] A. Salman, U. Sharaha, E. Rodriguez-Diaz, et al., "Detection of antibiotic resistant: *Escherichia coli* bacteria using infrared microscopy and advanced multivariate analysis," *Analyst*, vol. 142, pp. 2136–2144, 2017.
[145] M. Drancourt, A. Michel-Lepage, S. Boyer, and D. Raoult, "The point-of-care laboratory in clinical microbiology," *Clin. Microbiol. Rev.*, vol. 29, pp. 429–447, 2016.

[146] O. Pashchenko, T. Shelby, T. Banerjee, and S. Santra, "A comparison of optical, electrochemical, magnetic, and colorimetric point-of-care biosensors for infectious disease diagnosis," *ACS Infect. Dis.*, vol. 4, pp. 1162–1178, 2018.

[147] M. R. Pulido, M. García-Quintanilla, R. Martín-Peña, J. M. Cisneros, and M. J. McConnell, "Progress on the development of rapid methods for antimicrobial susceptibility testing," *J. Antimicrob. Chemother.*, vol. 68, pp. 2710–2717, 2013.

[148] A. Drayton, K. Li, M. Simmons, C. Reardon, and T. Krauss, "Performance limitations of resonant refractive index sensors with low-cost components," *Under Review*, https://doi.org/10.1364/OE.400236.